

RESEARCH

Onset, timing, and exposure therapy of stress disorders: mechanistic insight from a mathematical model of oscillating neuroendocrine dynamics

Lae Kim[†], Maria D'Orsogna[†] and Tom Chou^{*}

*Correspondence:

tomchou@ucla.edu

³Dept. of Biomathematics, Univ of California, Los Angeles, Los Angeles, USA

Full list of author information is available at the end of the article

[†]Equal contributor

Abstract

The hypothalamic-pituitary-adrenal (HPA) axis is a neuroendocrine system that regulates numerous physiological processes. Disruptions in the activity of the HPA axis are correlated with many stress-related diseases such as post-traumatic stress disorder (PTSD) and major depressive disorder. In this paper, we characterize “normal” and “diseased” states of the HPA axis as basins of attraction of a dynamical system describing the inhibition of peptide hormones such as corticotropin-releasing hormone (CRH) and adrenocorticotrophic hormone (ACTH) by circulating glucocorticoids such as cortisol (CORT). In addition to including key physiological features such as ultradian oscillations in cortisol levels and self-upregulation of CRH neuron activity, our model distinguishes the relatively slow process of cortisol-mediated CRH biosynthesis from rapid trans-synaptic effects that regulate the CRH secretion process. Crucially, we find that the slow regulation mechanism mediates external stress-driven transitions between the stable states in novel, intensity, duration, and timing-dependent ways. These results indicate that the *timing* of traumatic events may be an important factor in determining if and how patients will exhibit hallmarks of stress disorders. Our model also suggests a mechanism whereby exposure therapy of stress disorders such as PTSD may act to normalize downstream dysregulation of the HPA axis.

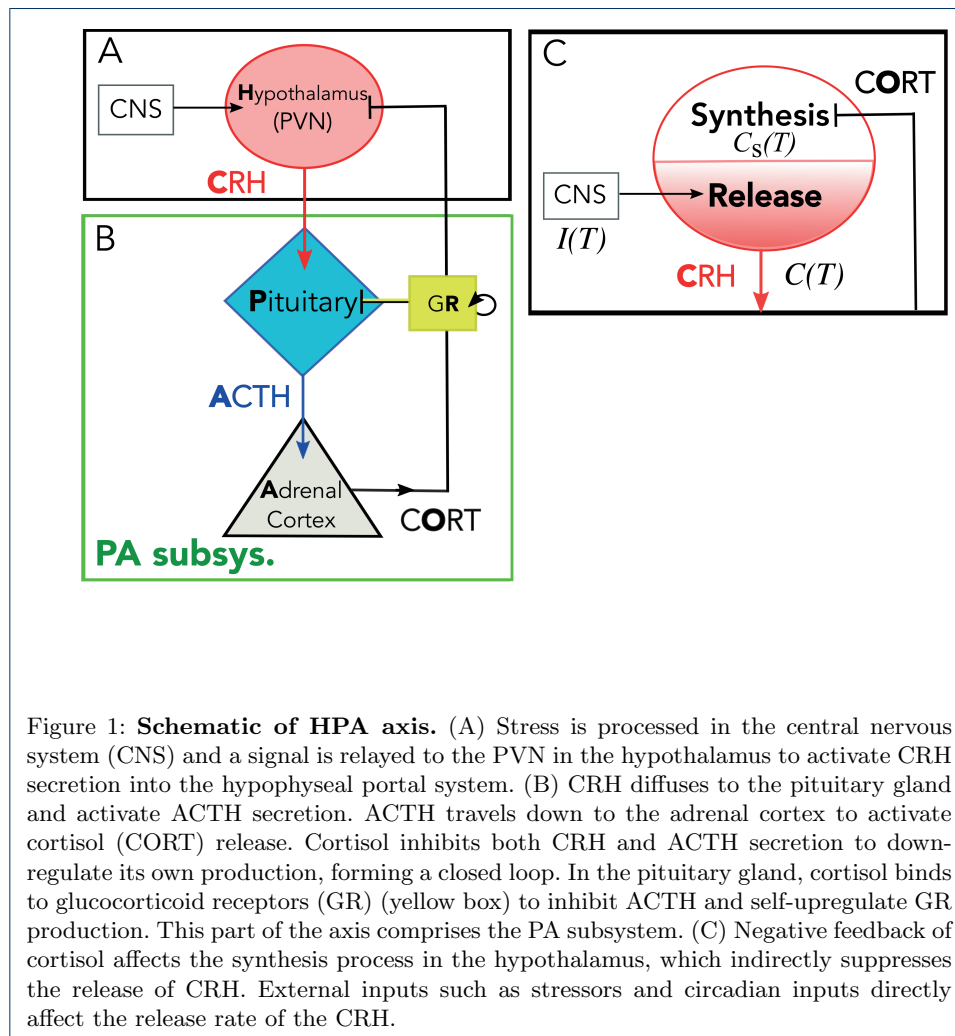
Keywords:

HPA-axis; PTSD; Stress Disorders; Dynamical system

1 Introduction

2 Stress is an essential component of an organism's attempt to adjust its internal
3 state in response to environmental change. The experience, or even the percep-
4 tion of physical and/or environmental change, induces stress responses such as the
5 secretion of glucocorticoids hormones (CORT) – cortisol in humans and corticos-
6 terone in rodents – by the adrenal gland. The adrenal gland is one component
7 of the hypothalamic-pituitary-adrenal (HPA) axis, a collection of interacting neu-
8 roendocrine cells and endocrine glands that play a central role in stress response.
9 The basic interactions involving the HPA axis are shown in Fig. 1. The paraven-
10 tricular nucleus (PVN) of the hypothalamus receives synaptic inputs from various
11 neural pathways via the central nervous system that are activated by both cog-
12 nitive and physical stressors. Once stimulated, CRH neurons in the PVN secrete

13 corticotropin-releasing hormone (CRH), which then stimulates the anterior pitu-
14 itary gland to release adrenocorticotropin hormone (ACTH) into the bloodstream.
15 ACTH then activates a complex signaling cascade in the adrenal cortex, which ul-
16 timately releases glucocorticoids (Fig. 1B). In return, glucocorticoids exert a negative
17 feedback on the hypothalamus and pituitary, suppressing CRH and ACTH release
18 and synthesis in an effort to return them to baseline levels. Classic stress responses
19 include transient increases in levels of CRH, ACTH, and cortisol. The basic compo-
20 nents and organization of the vertebrate neuroendocrine stress axis arose early in
21 evolution and the HPA axis, in particular, has been conserved across mammals [1].



22 Dysregulation in the HPA axis is known to correlate with a number of stress-
23 related disorders. Increased cortisol (hypercortisolism) is associated with major de-
24 pressive disorder (MDD) [2, 3], while decreased cortisol (hypocortisolism) is a fea-
25 ture of post-traumatic stress disorder (PTSD), post infectious fatigue, and chronic
26 fatigue syndrome (CFS) [4–7]. Since PTSD develops in the aftermath of extreme
27 levels of stress experienced during traumatic incidents like combat, sexual abuse, or
28 life-threatening accidents, its progression may be strongly correlated with disrupt-

tion of the HPA axis caused by stress response. For example, lower peak and nadir cortisol levels were found in patients with combat-related PTSD [8].

Mathematical models of the HPA axis have been previously formulated in terms of dynamical systems of ordinary differential equations (ODEs) [9–12] or delay differential equations (DDEs) [13–15] that describe the time-evolution of the key regulating hormones of the HPA axis: CRH, ACTH, and cortisol. These models [13, 14, 16] incorporate positive self-regulation of glucocorticoid receptor expression in the pituitary, which may generate bistability in the dynamical structure of the model [17]. Of the two stable equilibrium states, one is characterized by higher levels of cortisol and is identified as the “normal” state. The other is characterized by lower levels of cortisol and can be interpreted as one of the “diseased” states associated with *hypocortisolism*. Stresses that affect the activity of neurons in the PVN are described as perturbations to endogenous CRH secretion activity. Depending on the length and magnitude of the stress input, the system may or may not shift from the basin of attraction of the normal steady state towards that of the diseased one. If such a transition does occur, it may be interpreted as the onset of disease. A later model [16] describes the effect of stress on the HPA axis as a gradual change in the parameter values representing the maximum rate of CRH production and the strength of the negative feedback activity of cortisol. Changes in cortisol secretion pattern are assumed to arise from anatomical changes that are mathematically represented as changes to the corresponding parameter values [16].

Both classes of models imply qualitatively different time courses of disease progression [16, 17]. The former suggests that the abnormal state is a pre-existing basin of attraction of a dynamical model that stays dormant until a sudden transition is triggered by exposure to trauma [17]. In contrast, the latter assumes that the abnormal state is reached by the slow development of structural changes in physiology due to the traumatic experience [16]. Although both models [16, 17] describe changes in hormonal levels experienced by PTSD patients, they both fail to exhibit stable ultradian oscillations in cortisol, which is known to play a role in determining the responsiveness of the HPA axis to stressors [18].

In this study, we consider a number of distinctive physiological features of the HPA axis that give a more complete picture of the dynamics of stress disorders and that have not been considered in previous mathematical models. These include the effects of intrinsic ultradian oscillations on HPA dysregulation, distinct rapid and slow feedback actions of cortisol, and the correlation between HPA imbalance and disorders induced by external stress. As with the majority of hormones released by the body, cortisol levels undergo a circadian rhythm, starting low during night sleep, rapidly rising and reaching its peak in the early morning, then gradually falling throughout the day. Superposed on this slow diurnal cycle is an ultradian rhythm consisting of approximately hourly pulses. CRH, ACTH, and cortisol are all secreted episodically, with the pulses of ACTH slightly preceding those of cortisol [19].

As for many other hormones such as gonadotropin-releasing hormone (GnRH), insulin, and growth hormone (GH), the ultradian release pattern of glucocorticoids is important in sustaining normal physiological functions, such as regulating gene expression in the hippocampus [20]. It is unclear what role oscillations play in

75 homeostasis, but the time of onset of a stressor in relation to the phase of the
76 ultradian oscillation has been shown to influence the physiological response elicited
77 by the stressor [21].

78 To distinguish the rapid and slow actions of cortisol, we separate the dynamics
79 of biosynthesis of CRH from its secretion process, which operate over very different
80 timescales [22]. While the two processes are mostly independent from each other, the
81 rate of CRH secretion should depend on the synthesis process since CRH peptides
82 must be synthesized first before being released (Fig. 1C). On the other hand, the rate
83 of CRH peptide synthesis is influenced by cortisol levels, which in turn, are regulated
84 by released CRH levels. We will investigate how the separation and coupling of these
85 two processes can allow stress-induced dysregulations of the HPA axis.

86 The mathematical model we derive incorporates the above physiological features
87 and reflects the basic physiology of the HPA axis associated with delays in signal-
88 ing, fast and slow negative feedback mechanisms, and CRH self-upregulation [23].
89 Within an appropriate parameter regime, our model exhibits two distinct stable
90 *oscillating* states, of which one is marked by a larger oscillation amplitude and
91 a higher base cortisol level than the other. These two states will be referred to
92 as normal and diseased states. Our interpretation is reminiscent of the two-state
93 dynamical structure that arises in the classic Fitzhugh-Nagumo model of a single
94 neuron, in which resting and spiking states emerge as bistable modes of the model
95 [24], or in models of neuronal networks where an “epileptic brain” is described in
96 terms of the distance between a normal and a seizure attractor in phase-space [25].

97 **Models**

98 Models of HPA dynamics [13, 14, 16, 17, 26] are typically expressed in terms of
99 ordinary differential equations (ODEs):

$$\frac{dC}{dT} = p_C I(T) f_C(O) - d_C(C), \quad (1)$$

$$\frac{dA}{dT} = p_A C f_A(OR, O) - d_A(A), \quad (2)$$

$$\frac{dO}{dT} = p_O A(T) - d_O(O), \quad (3)$$

$$\frac{dR}{dT} = p_{RG} R(OR) - d_R(R), \quad (4)$$

100 where $C(T)$, $A(T)$, and $O(T)$ denote the plasma concentrations of CRH, ACTH,
101 and cortisol at time T , respectively. $R(T)$ represents the availability of glucocor-
102 ticoid receptor (GR) in the anterior pituitary. The amount of cortisol bound GR
103 is typically in quasi-equilibrium so concentration of the ligand-receptor complex
104 is approximately proportional to the product $O(T)R(T)$ [17]. The parameters p_α
105 ($\alpha \in \{C, A, O, R\}$) relate the production rate of each species α to specific factors
106 that regulate the rate of release/synthesis. External stresses that drive CRH release
107 by the PVN in the hypothalamus are represented by the input signal $I(T)$. The func-
108 tion $f_C(O)$ describes the negative feedback of cortisol on CRH levels in the PVN
109 while $f_A(OR, O)$ describes the negative feedback of cortisol or cortisol-GR complex

110 (at concentration $O(T)R(T)$) in the pituitary. Both are mathematically character-
111 ized as being positive, decreasing functions so that $f_{A,C}(\cdot) \geq 0$ and $f'_{A,C}(\cdot) < 0$. On
112 the other hand, the function $g_R(OR)$ describes the self-upregulation effect of the
113 cortisol-GR complex on GR production in the anterior pituitary [27]. In contrast
114 to $f_{A,C}(\cdot)$, $g_R(\cdot)$ is a positive but increasing function of OR so that $g_R(\cdot) \geq 0$ and
115 $g'_R(\cdot) > 0$. Finally, the degradation functions $d_\alpha(\cdot)$ describe how each hormone and
116 receptor is cleared and may be linear or nonlinear.

117 Without including the effects of the glucocorticoid receptor (neglecting Eq. 4 and
118 assuming $f_A(OR, O) = f_A(O)$ in Eq. 2), Eqs. 1-3 form a rudimentary “minimal”
119 model of the HPA axis [9, 28]. If $f_{A,C}(\cdot)$ are Hill-type feedback functions depen-
120 dent only on $O(T)$ and $d_\alpha(\cdot)$ are linear, a unique global stable point exists. This
121 equilibrium point transitions to a limit cycle through a Hopf bifurcation but only
122 within nonphysiological parameter regimes [9]. The inclusion of GR and its self-
123 upregulation in the anterior pituitary [17] creates two stable equilibrium states of
124 the system, but still does not generate oscillatory behavior. More recent studies
125 extend the model (represented by Eq. 1-4) to include nonlinear degradation [16] or
126 constant delay to account for delivery of ACTH and synthesis of glucocorticoid in
127 the adrenal gland [13]. These two extended models exhibit only one intrinsic circa-
128 dian [16] or ultradian [13] oscillating cycle for any given set of parameter values,
129 precluding the interpretation of normal and diseased states as bistable oscillating
130 modes of the model.

131 Here, we develop a new model of the HPA axis by first adapting previous work
132 [13] where a physiologically-motivated delay was introduced into Eq. 3, giving rise
133 to the observed ultradian oscillations [13]. We then improve the model by dis-
134 tinguishing the relatively slow mechanism underlying the cortisol-mediated CRH
135 biosynthesis from the rapid trans-synaptic effects that regulate the CRH secretion
136 process. This allows us to decompose the dynamics into slow and fast components.
137 Finally, self-upregulation of CRH release is introduced which allows for bistabil-
138 ity. These ingredients can be realistically combined in a way that leads to novel,
139 clinically identifiable features and are systematically developed below

140 Ultradian rhythm and time delay

141 Experiments on rats show a 3-6 minute inherent delay in the response of the adrenal
142 gland to ACTH [29]. Moreover, in experiments performed on sheep [30], persistent
143 ultradian oscillations were observed even after surgically removing the hypothala-
144 mus, implying that oscillations are inherent to the PA subsystem. Since oscillations
145 can be induced by delays, we assume, as in Walker *et al.* [13], a time delay T_d in the
146 ACTH-mediated activation of cortisol production downstream of the hypothalamus.
147 Eq. 3 is thus modified to

$$\frac{dO}{dT} = p_O A(T - T_d) - d_O O. \quad (5)$$

148 Walker *et al.* [13] show that for fixed physiological levels of CRH, the solution to
149 Eqs. 2, 4 and 5 leads to oscillatory $A(T)$, $O(T)$, and $R(T)$. In order to describe the
150 observed periodic cortisol levels in normal and diseased states, the model requires

151 *two* oscillating stable states. We will see that dual oscillating states arise within
152 our model when the delay in ACTH-mediated activation of cortisol production is
153 coupled with other known physiological processes.

154 Synthesis of CRH

155 CRH synthesis involves various pathways, including CRH gene transcription and
156 transport of packaged CRH from the cell body (soma) to their axonal terminals
157 where they are stored prior to release. Changes in the steady state of the synthesis
158 process typically occur on a timescale of minutes to hours. On the other hand, the
159 secretory release process depends on changes in membrane potential at the axonal
160 terminal of CRH neurons, which occur over millisecond to second timescales.

161 To model the synthesis and release process separately, we distinguish two com-
162 partments of CRH: the concentration of stored CRH within CRH neurons will be
163 denoted $C_s(T)$, while levels of released CRH in the portal vein outside the neurons
164 will be labeled $C(T)$ (Fig. 1C). Newly synthesized CRH will first be stored, thus
165 contributing to C_s . We assume that the stored CRH level C_s relaxes toward a target
166 value set by the function $C_\infty(O)$:

$$\frac{dC_s}{dT} = \frac{C_\infty(O) - C_s}{T_C}. \quad (6)$$

167 Here, T_C is a characteristic time constant and $C_\infty(O)$ is the *cortisol-dependent*
168 target level of stored CRH. Eq. 6 also assumes that the relatively small amounts of
169 CRH released into the bloodstream do not significantly deplete the C_s pool. Note
170 that the effects induced by changing cortisol levels are immediate as the production
171 term $C_\infty(O)/T_C$ is adjusted instantaneously to current cortisol levels. Our model
172 thus does not exclude cortisol rapidly acting on the initial transcription activity,
173 as suggested by CRH hnRNA (precursor mRNA) measurements [31]. On the other
174 hand, the time required to reach the steady state for the completely synthesized
175 CRH peptide will depend on the characteristic time scale constant T_C . Ideally,
176 T_C should be estimated from measurements of the pool size of releasable CRH
177 at the axonal terminals. To best of our knowledge, there are currently no such
178 measurements available, so we base our estimation on mRNA level measurements.
179 We believe this is a better representation of releasable CRH than hnRNA levels since
180 mRNA synthesis is a further downstream process. Previous studies have shown that
181 variations in CRH mRNA due to changes in cortisol levels take at least twelve hours
182 to detect [32]. Therefore, we estimate $T_C \gtrsim 12\text{hrs} = 720\text{min}$. The negative feedback
183 of cortisol on CRH levels thus acts through the production function $C_\infty(O)$ on
184 the relatively slow timescale T_C . To motivate the functional form of $C_\infty(O)$, we
185 invoke experiments on rats whose adrenal glands had been surgically removed and
186 in which glucocorticoid levels were subsequently kept fixed (by injecting exogenous
187 glucocorticoid) for 5-7 days [22, 33]. The measured CRH mRNA levels in the PVN
188 were found to decrease exponentially with the level of administered glucocorticoid
189 [22, 33]. Assuming the amount of releasable CRH is proportional to the amount of
190 measured intracellular CRH mRNA, we can approximate $C_\infty(O)$ as a decreasing
191 exponential function of cortisol level O .

192 Secretion of CRH

193 To describe the CRH secretion, we consider the following three factors: synaptic
194 inputs to CRH cells in the PVN, availability of releasable CRH peptide, and self-
195 upregulation of CRH release.

CRH secretion activity is regulated by synaptic inputs received by the PVN from multiple brain regions including limbic structures like the hippocampus and the amygdala, that are activated during stress. It has been reported that for certain types of stressors, these synaptic inputs are modulated by cortisol independent of, or parallel to, its regulatory function on CRH synthesis activity [34]. On the other hand, a series of studies [35–37] showed that cortisol did not affect the basal spiking activity of the PVN. We model the overall synaptic input, denoted by $I(T)$ in Eq. 1, as follows

$$I(T) = I_{\text{base}} + I_{\text{ext}}(T), \quad (7)$$

196 where I_{base} and $I_{\text{ext}}(T)$ represent the basal firing rate and stress-dependent synaptic
197 input of the PVN, respectively. As the effect of cortisol on the synaptic input during
198 stress is specific to type of stressor [38–40], we assume $I_{\text{ext}}(T)$ to be independent
199 of O for simplicity and generality. Possible implications of cortisol dependent input
200 function $I_{\text{ext}}(T, O)$ on model behavior will be discussed in the Additional File.

201 The secretion of CRH will also depend upon the amount of stored *releasable* CRH,
202 $C_s(T)$, within the neuron and inside the synaptic vesicles. Therefore, C_s can also
203 be factored into Eq. 1 through a source term $h(C_s)$ which describes the amount
204 of CRH released per unit of action potential activity of CRH neurons. Finally,
205 it has been hypothesized that CRH enhances its own release [23], especially when
206 external stressors are present. The enhancement of CRH release by CRH is mediated
207 by activation of the membrane-bound G-protein-coupled receptor CRHR-1 whose
208 downstream signaling pathways operate on timescales from milliseconds to seconds
209 [41, 42]. Thus, self-upregulation of CRH release can be modeled by including a
210 positive and increasing function $g_C(C)$ in the source term in Eq. 1.

211 Combining all these factors involved in regulating the secretion process, we can
212 rewrite Eq. 1 by replacing $f_C(O)$ with $h(C_s)g_C(C)$ as follows

$$\frac{dC}{dT} = p_C I(T) h(C_s) g_C(C) - d_C C. \quad (8)$$

213 In this model (represented by Eqs. 6, 8, 2, 5, and 4), cortisol no longer *directly* sup-
214 presses CRH levels, rather, it decreases CRH synthesis through Eq. 6, in turn sup-
215 pressing C_s . The combination $h(C_s)g_C(C)$ in Eq. 8 indicates the release rate of
216 stored CRH decreases when either C_s or C decreases. We assume that inputs into
217 the CRH neurons modulate the overall release process with weight p_C .

218 Complete delay-differential equation model

219 We are now ready to incorporate the mechanisms described above into a new, more
220 comprehensive mathematical model of the HPA axis, which, in summary, includes

- 221 (i) A delayed response of the adrenal cortex to cortisol (Eq. 5).

222 (ii) A slow time-scale negative feedback by cortisol on CRH synthesis (through
223 the $C_\infty(O)$ production term in Eq. 6).

224 (iii) A fast-acting positive feedback of stored and circulating CRH on CRH release
225 (through the $h(C_s)g_C(C)$ term in Eq. 8);

226 Our complete mathematical model thus consists of Eqs. 2, 4, 5, 6, and 8. We hence-
227 forth assume $f_A(OR, O) = f_A(OR)$ depends on only the cortisol-GR complex and
228 use Hill-type functions for $f_A(OR)$ and $g_R(OR)$ [13, 14, 16, 17]. Our full theory is
229 characterized by the following system of delay differential equations:

$$\frac{dC_s}{dT} = \frac{C_\infty(O) - C_s}{T_C}, \quad (9)$$

$$\frac{dC}{dT} = p_C I(T) h(C_s) g_C(C) - d_C C, \quad (10)$$

$$\frac{dA}{dT} = p_A C \left(\frac{K_A}{K_A + OR} \right) - d_A A, \quad (11)$$

$$\frac{dO}{dT} = p_O A(T - T_d) - d_O O, \quad (12)$$

$$\frac{dR}{dT} = p_R \left(1 - \frac{\mu_R K_R^2}{K_R^2 + (OR)^2} \right) - d_R R. \quad (13)$$

230 The parameters $K_{A,R}$ represent the level of A and R at which the negative or
231 positive effect are at their half maximum and $1 - \mu_R$ represents the basal production
232 rate for GR when $OR = 0$.

233 Of all the processes modeled, we will see that the slow negative feedback will
234 be crucial in mediating transitions between stable states of the system. The slow
235 dynamics will allow state variables to cross basins of attraction associated with each
236 of the stable states.

237 Nondimensionalization

238 To simplify the further development and analysis of our model, we nondimensional-
239 ize Eqs. 9-13 by rescaling all variables and parameters in a manner similar to that
240 of Walker *et al.* [13], as explicitly shown in the Additional File. We find

$$\frac{dc_s}{dt} = \frac{c_\infty(o) - c_s}{t_c}, \quad (14)$$

$$\frac{dc}{dt} = q_0 I(t) h(c_s) g_c(c) - q_2 c, \quad (15)$$

$$\frac{da}{dt} = \frac{c}{1 + p_2(or)} - p_3 a, \quad (16)$$

$$\frac{do}{dt} = a(t - t_d) - o, \quad (17)$$

$$\frac{dr}{dt} = \frac{(or)^2}{p_4 + (or)^2} + p_5 - p_6 a, \quad (18)$$

241 where c_s, c, a, r, o are the dimensionless versions of the original concentrations
242 C_s, C, A, R, O , respectively. The dimensionless delay in activation of cortisol pro-
243 duction by ACTH is now denoted t_d . All dimensionless parameters q_i, p_i, t_d , and

244 t_c are combinations of the physical parameters and are explicitly given in the Ad-
 245 dditional File. The functions $c_\infty(o)$, $h(c_s)$, and $g_c(c)$ are dimensionless versions of
 246 $C_\infty(O)$, $h(C_s)$, and $g_C(C)$, respectively, and will be chosen phenomenologically to
 247 be

$$\begin{aligned} c_\infty(o) &= \bar{c}_\infty + e^{-bo}, \\ h(c_s) &= 1 - e^{-kc_s}, \\ g_c(c) &= 1 - \frac{\mu_c}{1 + (q_1c)^n}. \end{aligned} \quad (19)$$

248 The form of $c_\infty(o)$ is based on the above-mentioned exponential relation observed
 249 in adrenalectomized rats [22, 33]. The parameters \bar{c}_∞ and b represent the minimum
 250 dimensionless level of stored CRH and the decay rate of the function, respectively.
 251 How the rate of CRH release increases with c_s is given by the function $h(c_s)$. Since
 252 the amount of CRH packaged in release vesicles is likely regulated, we assume
 253 $h(c_s)$ saturates at high c_s . The choice of a decreasing form for $c_\infty(o)$ implies that
 254 increasing cortisol levels will decrease the target level (or production rate) of c_s in
 255 Eq. 14. The reduced production of c_s will then lead to a smaller $h(c_s)$ and ultimately
 256 a reduced release source for c (Eq. 15). As expected, the overall effect of increasing
 257 cortisol is a decrease in the release rate of CRH. Finally, since the upregulation of
 258 CRH release by circulating CRH is mediated by binding to CRH receptor, $g_c(c)$
 259 will be chosen to be a Hill-type function, with Hill-exponent n , similar in form to
 260 the function $g_R(OR)$ used in Eqs. 13 and 18. The parameter $1 - \mu_c$ represents the
 261 basal release rate of CRH relative to the maximum release rate and q_1^{-1} represents
 262 the normalized CRH level at which the positive effect is at half-maximum.

263 Fast-slow variable separation and bistability

264 Since we assume the negative feedback effect of cortisol on synthesis of CRH operates
 265 over the longest characteristic timescale t_c in the problem, the full model must be
 266 studied across two separate timescales, a *fast timescale* t , and a *slow timescale*
 267 $\tau = t/t_c \equiv \varepsilon t$. The full model (Eqs. 14-18) can be succinctly written in the form

$$\frac{dc_s}{dt} = \varepsilon(c_\infty(o) - c_s), \quad (20)$$

$$\frac{d\mathbf{x}}{dt} = \mathbf{F}(c_s, \mathbf{x}), \quad (21)$$

268 where $\mathbf{x} = (c, a, o, r)$ is the vector of fast dynamical variables, and $\mathbf{F}(c_s, \mathbf{x})$ denotes
 269 the right-hand-sides of Eqs. 15-18. We refer to the fast dynamics described by
 270 $d\mathbf{x}/dt = \mathbf{F}(c_s, \mathbf{x})$ as a *fast flow*. In the $\varepsilon \rightarrow 0$ limit, it is also easy to see that to
 271 lowest order c_s is a constant across the fast timescale and is a function of only the
 272 slow variable τ .

273 Under this timescale separation, the first component of Eq. 21 (Eq. 15) can be
 274 written as

$$\frac{dc}{dt} = q(c_s(\tau), I)g_c(c) - q_2c, \quad (22)$$

275 where $q(c_s(\tau), I) \equiv q_0 I h(c_s(\tau)) = q_0 I (1 - e^{-k c_s(\tau)})$ is a function of $c_s(\tau)$ and I .
 276 Since c_s is a function only of the slow timescale τ , q can be viewed as a bifurcation
 277 parameter controlling, over short timescales, the fast flow described by Eq. 22. Once
 278 $c(t)$ quickly reaches its non-oscillating quasi-equilibrium value defined by $dc/dt =$
 279 $qg_c(c) - q_2c = 0$, it can be viewed as a parametric term in Eq. 16 of the pituitary-
 280 adrenal (PA) subsystem.

281 Due to the nonlinearity of $g_c(c)$, the equilibrium value $c(q)$ satisfying $qg_c(c) = q_2c$
 282 may be multi-valued depending on q , as shown in Figs. 2A and 2B. For certain values
 283 of the free parameters, such as $n, 1 - \mu_c$, and q_1 , bistability can emerge through a
 284 saddle-node bifurcation with respect to the bifurcation parameter q . Fig. 2B shows
 285 the bifurcation diagram, *i.e.*, the nullcline of c defined by $qg_c(c) = q_2c$.

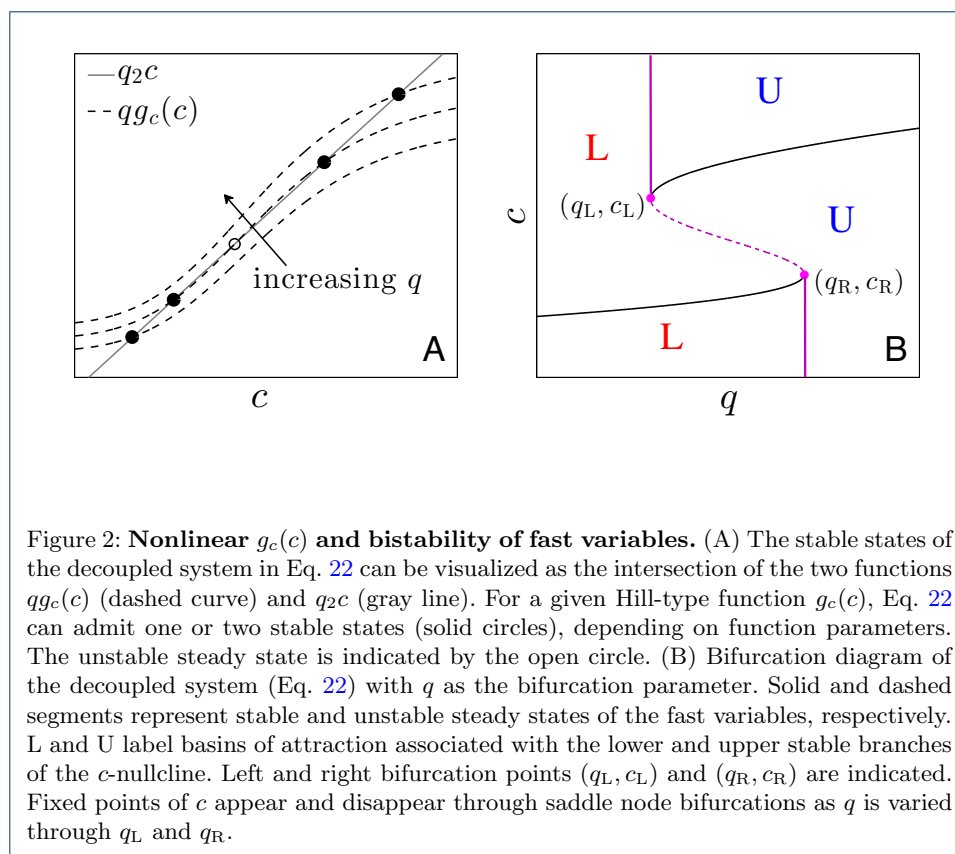
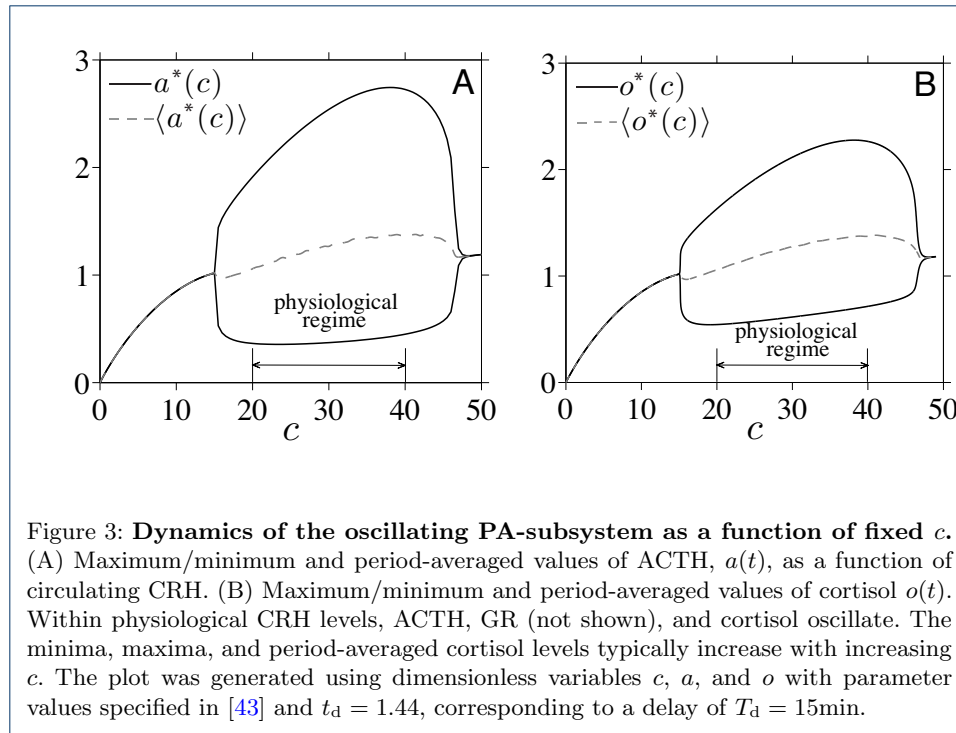


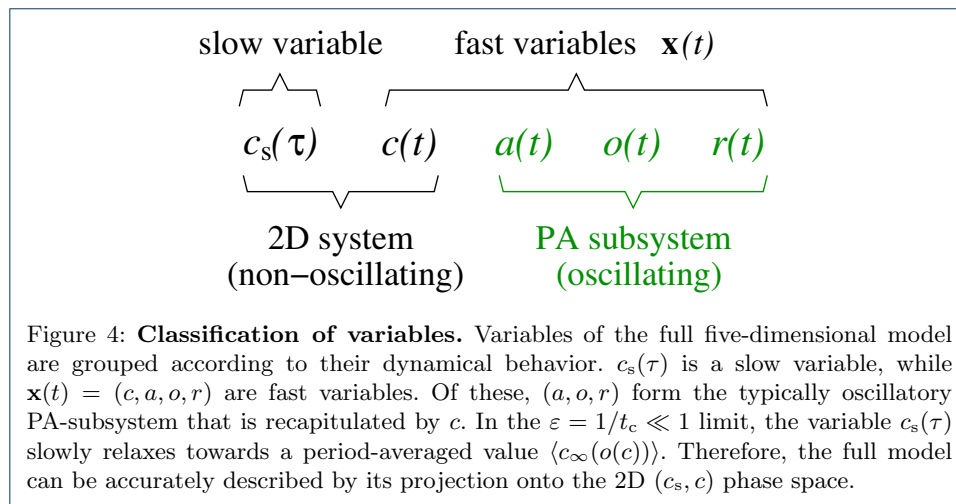
Figure 2: **Nonlinear $g_c(c)$ and bistability of fast variables.** (A) The stable states of the decoupled system in Eq. 22 can be visualized as the intersection of the two functions $qg_c(c)$ (dashed curve) and q_2c (gray line). For a given Hill-type function $g_c(c)$, Eq. 22 can admit one or two stable states (solid circles), depending on function parameters. The unstable steady state is indicated by the open circle. (B) Bifurcation diagram of the decoupled system (Eq. 22) with q as the bifurcation parameter. Solid and dashed segments represent stable and unstable steady states of the fast variables, respectively. L and U label basins of attraction associated with the lower and upper stable branches of the c -nullcline. Left and right bifurcation points (q_L, c_L) and (q_R, c_R) are indicated. Fixed points of c appear and disappear through saddle node bifurcations as q is varied through q_L and q_R .

286 For equilibrium values of c lying within a certain range, the PA-subsystem can
 287 exhibit a limit cycle in (a, o, r) [13] that we express as $(a^*(\theta; c), o^*(\theta; c), r^*(\theta; c))$,
 288 where $\theta = 2\pi t/t_p(c)$ is the phase along the limit cycle. The dynamics of the PA-
 289 subsystem depicted in Fig. 3 indicate the range of c values that admit limit cycle
 290 behavior for (a, o, r) , while the fast c -nullcline depicted in Fig. 2B restricts the range
 291 of bistable c values. Thus, bistable states that also support oscillating (a, o, r) are
 292 possible only for values of c that satisfy both criteria.

293 Since in the $\varepsilon \rightarrow 0$ limit, circulating CRH only feeds forward into a, o , and r , a
 294 complete description of all the fast variables can be constructed from just c which
 295 obeys Eq. 22. Therefore, to visualize and approximate the dynamics of the full five-
 296 dimensional model, we only need to consider the 2D projection onto the fast c and



297 slow c_s variable. A summary of the time-separated dynamics of the variables in our
 298 model is given in Fig. 4.



298

299 To analyze the evolution of the slow variable $c_s(\tau)$, we write our equations in
 300 terms of $\tau = \varepsilon t$:

$$\frac{dc_s}{d\tau} = (c_\infty(o) - c_s), \quad (23)$$

$$\varepsilon \frac{d\mathbf{x}}{d\tau} = \mathbf{F}(c_s, \mathbf{x}). \quad (24)$$

301 In the $\varepsilon \rightarrow 0$ limit, the “outer solution” $\mathbf{F}(c_s, \mathbf{x}) \approx 0$ simply constrains the system to
 302 be on the fast c -nullcline defined by $qg_c(c) = q_2c$. The slow evolution of $c_s(\tau)$ along
 303 the fast c -nullcline depends on the value of the fast variable $o(t)$ through $c_\infty(o)$. To
 304 close the slow flow subsystem for $c_s(\tau)$, we fix c to its equilibrium value as defined
 305 by the fast subsystem and approximate $c_\infty(o(c))$ in Eq. 23 by its period-averaged
 306 value

$$\langle c_\infty(c) \rangle \equiv \int_0^{2\pi} c_\infty(o^*(\theta; c)) \frac{d\theta}{2\pi} = \bar{c}_\infty + \int_0^{2\pi} e^{-bo^*(\theta; c)} \frac{d\theta}{2\pi}. \quad (25)$$

307 Since o^* increases with c , $\langle c_\infty(c) \rangle$ is a decreasing function of c under physiological
 308 parameter regimes. This period-averaging approximation allows us to relate the
 309 evolution of $c_s(\tau)$ in the slow subsystem directly to c . The evolution of the slow
 310 subsystem is approximated by the closed (c_s, c) system of equations

$$\frac{dc_s}{d\tau} = \langle c_\infty(c) \rangle - c_s, \quad (26)$$

$$0 = q_0 h(c_s) I(t) g_c(c) - q_2 c. \quad (27)$$

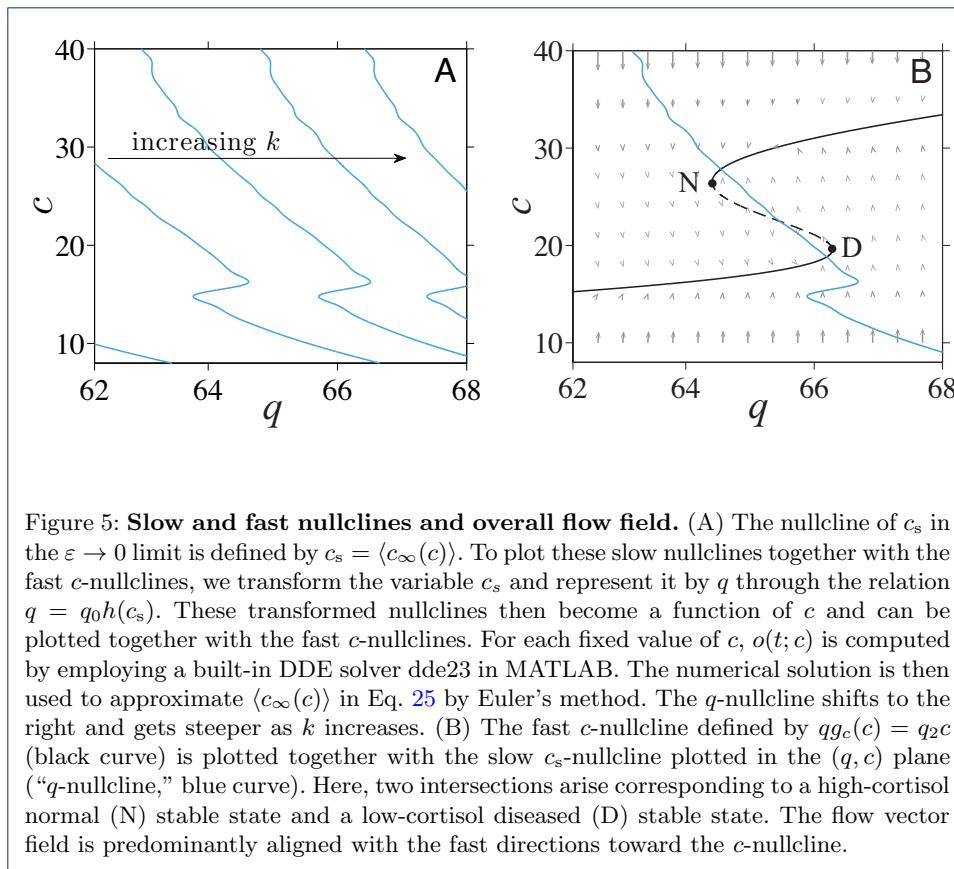
311 with $\langle c_\infty(c) \rangle$ evaluated in Eq. 25. By self-consistently solving Eqs. 26 and 27, we
 312 can estimate trajectories of the full model when they are near the c -nullcline in the
 313 2D (c_s, c) -subsystem. We will verify this in the following section.

314 Nullcline structure and projected dynamics

315 The separation of timescales results in a natural description of the fast c -nullcline in
 316 terms of the parameter q (Fig. 2) and the slow c_s -nullcline (defined by the relation
 317 $c_s = \langle c_\infty(c) \rangle$ relating c_s to c) in terms of c . However, the c -nullcline is plotted
 318 in the (q, c) -plane while the c_s -nullcline is defined in the (c, c_s) -plane. To plot the
 319 nullclines together, we relate the equilibrium value of c_s , $\langle c_\infty(c) \rangle$, to the q coordinate
 320 through the monotonic relationship $q(c_s) = q_0 I h(\langle c_\infty(c) \rangle) = q_0 I (1 - e^{-k\langle c_\infty(c) \rangle})$
 321 and transform the c_s variable into the q parameter so that both nullclines can be
 322 plotted together in the (q, c) -plane. These transformed c_s -nullclines will be denoted
 323 “ q -nullclines.”

324 We assume a fixed basal stress input $I = 1$ and plot the q -nullclines in Fig. 5A
 325 for increasing values of k , the parameter governing the sensitivity of CRH release
 326 to stored CRH. From the form $h(\langle c_\infty(c) \rangle) = (1 - e^{-k\langle c_\infty(c) \rangle})$, both the position and
 327 the steepness of the q -nullcline in (q, c) -space depend strongly on k . Fig. 5B shows a
 328 fast c -nullcline and a slow q -nullcline (transformed c_s -nullcline) intersecting at both
 329 stable branches of the fast c -nullcline. Here, the flow field indicates that the 2D
 330 projected trajectory is governed by fast flow over most of the (q, c) -space.

331 How the fast and slow nullclines cross controls the long-term behavior of our model
 332 in the small ε limit. In general, the number of allowable nullcline intersections will
 333 depend on input level I and on parameters $(q_0, \dots, p_6, b, k, n, \mu_c, t_d)$. Other paramete-
 334 rs such as q_0 , q_1 , and μ_c appear directly in the fast equation for c and thus most
 335 strongly control the fast c -nullcline. Fig. 6A shows that for a basal stress input of

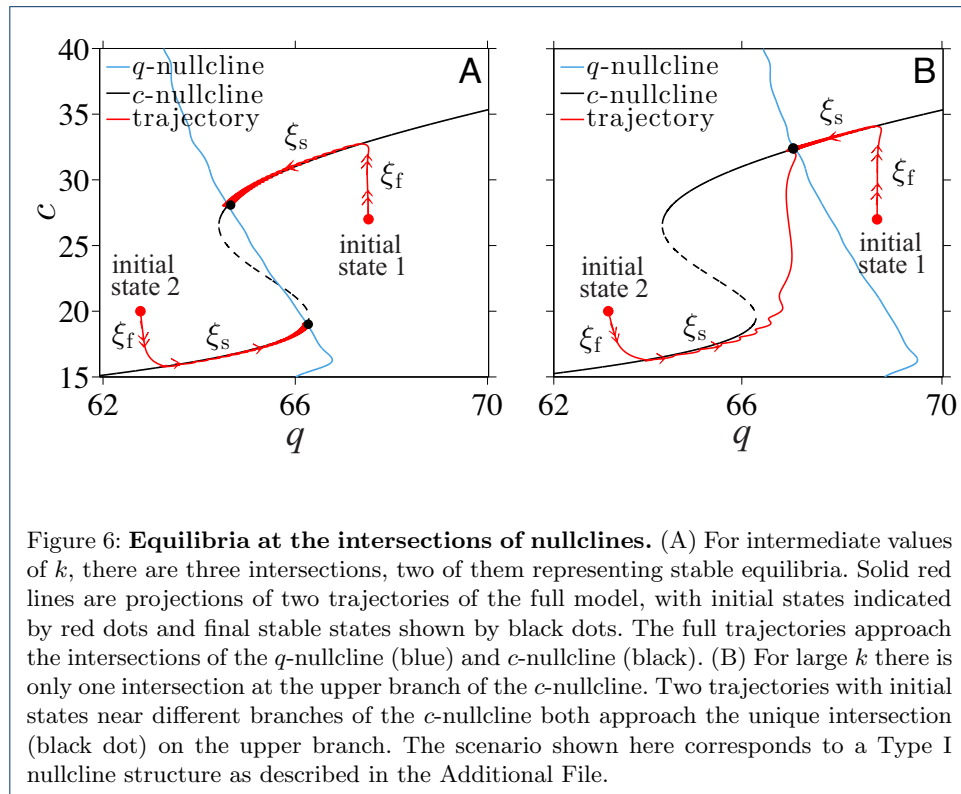


336 $I = 1$ and an intermediate value of k , the nullclines cross at both stable branches
 337 of the fast subsystem. As expected, numerical simulations of our full model show
 338 the fast variables (a, o, r) quickly reaching their oscillating states defined by the c -
 339 nullcline while the slow variable $q = q_0 I h(c_s)$ remains fairly constant. Independent
 340 of initial configurations that are not near the c -nullcline in (q, c) -space, trajecto-
 341 ries quickly jump to one of the stable branches of the c -nullcline with little motion
 342 towards the q -nullcline, as indicated by ξ_f in Fig. 6A.

343 Once near the c -nullcline, say when $|\mathbf{F}(c_s, \mathbf{x})| \ll \varepsilon$, the trajectories vary slowly
 344 according to Eqs. 23. Here, the slow variable c_s relaxes to its steady state value
 345 while satisfying the constraint $\mathbf{F}(c_s, \mathbf{x}) \approx 0$. In (q, c) -space, the system slowly
 346 slides along the c -nullcline towards the q -nullcline (the ξ_s paths in Fig. 6A). This
 347 latter phase of the evolution continues until the system reaches an intersection of
 348 the two nullclines, indicated by the filled dot, at which the reduced subsystem in c_s
 349 and c reaches equilibrium.

350 For certain values of k and if the fast variable c is bistable, the two nullclines
 351 may intersect within each of the two stable branches of the c -nullcline and yield
 352 the two distinct stable solutions shown in Fig. 6A. For large k , the two nullclines
 353 may only intersect on one stable branch of the c -nullcline as shown in Fig. 6B.
 354 Trajectories that start within the basin of attraction of the lower stable branch of
 355 the c -nullcline ("initial state 2" in Fig. 6B) will stay on this branch for a long time
 356 before eventually sliding off near the bifurcation point and jumping to the upper

357 stable branch. Thus, the long-term behavior of the full model can be described in
358 terms of the locations of the intersections of nullclines of the reduced system.



359 Results and Discussion

360 The dual-nullcline structure and existence of multiple states discussed above results
361 from the separation of slow CRH synthesis process and fast CRH secretion process.
362 This natural physiological separation of time scales ultimately gives rise to slow
363 dynamics along the fast c -nullcline during stress. The extent of this slow dynamics
364 will ultimately determine whether a transition between stable states can be induced
365 by stress. In this section, we explore how external stress-driven transitions mediated
366 by the fast-slow negative feedback depend on system parameters.

367 Changes in parameters that accompany trauma can lead to shifts in the position
368 of the nullclines. For example, if the stored CRH release process is sufficiently com-
369 promised by trauma (smaller k), the slow q -nullcline moves to the left, driving a
370 bistable or fully resistant organism into a stable diseased state. Interventions that
371 increase k would need to overcome hysteresis in order to restore normal HPA func-
372 tion. More permanent changes in parameters are likely to be caused by physical
373 rather than by psychological traumas since such changes would imply altered phys-
374 iology and biochemistry of the person. Traumatic brain injury (TBI) is an example
375 of where parameters can be changed permanently by physical trauma. The injury
376 may decrease the sensitivity of the pituitary to cortisol-GR complex, which can be
377 described by decreasing p_2 in our model. Such change in parameter would lead to
378 a leftward shift of the q -nullcline and an increased likelihood of hypocortisolism.

379 In the remainders of this work, we focus on how external stress inputs can by them-
380 selves induce stable but reversible transitions in HPA dynamics *without* changes in
381 physiological parameters. Specifically, we consider only temporary changes in $I(t)$
382 and consider the time-autonomous problem. Since the majority of neural circuits
383 that project to the PVN are excitatory [44], we assume external stress stimulates
384 CRH neurons to release CRH above its unit basal rate and that $I(t) = 1 + I_{\text{ext}}(t)$
385 ($I_{\text{base}} = 1$) with $I_{\text{ext}} \geq 0$.

386 To be more concrete in our analysis, we now choose our nullclines by specifying
387 parameter values. We estimate the values of many of the dimensionless parameters
388 by using values from previous studies, as listed in Table S1 in the Additional File.
389 Of the four remaining parameters, μ_c , q_0 , q_1 , and k , we will study how our model
390 depends on k while fixing μ_c , q_0 , and q_1 . Three possible nullcline configurations arise
391 according to the values of μ_c , q_0 , and q_1 and are delineated in the Additional File.
392 We have also implicitly considered only parameter regimes that yield oscillations in
393 the PA subsystem at the stable states defined by the nullcline intersections.

394 Given these considerations, we henceforth chose $\mu_c = 0.6$, $q_1 = 0.04$, and $q_0 = 77.8$
395 for the rest of our analysis. This choice of parameters is motivated in the Additional
396 File and corresponds to a so-called “Type I” nullcline structure. In this case, three
397 possibilities arise: one intersection on the lower stable branch of the c -nullcline if
398 $k < k_L$, two intersections if $k_L < k < k_R$ (Fig. 6A), and one intersection on the
399 upper stable branch of the c -nullcline if $k > k_R$ (Fig. 6B). For our chosen set of
400 parameters and a basal stress input $I = 1$, the critical values $k_L = 2.5 < k_R = 2.54$
401 are given by Eq. A3 in the Additional File.

402 Normal stress response

403 Activation of the HPA axis by acute stress culminates in an increased secretion
404 of all three main hormones of the HPA axis. Persistent hypersecretion may lead
405 to numerous metabolic, affective, and psychotic dysfunctions [45, 46]. Therefore,
406 recovery after stress-induced perturbation is essential to normal HPA function. We
407 explore the stability of the HPA axis by initiating the system in the upper of the two
408 stable points shown in Fig. 7A and then imposing a 120min external stress input
409 $I_{\text{ext}} = 0.1$. The HPA axis responds with an increase in the peak level of cortisol
410 before relaxing back to its original state after the stress is terminated (Fig. 7B).
411 This transient process is depicted in the projected (q, c) -space in Fig. 7A.

412 Upon turning on stress, the lumped parameter q and the slow nullcline shift to the
413 right by 10% since $q = q_0(1 + I_{\text{ext}})h(\langle c_\infty(c) \rangle)$ (see Fig. 7A). The trajectory will then
414 move rapidly upward towards the new value of c on the c -nullcline; afterwards, it
415 moves very slowly along the c -nullcline towards the shifted q -nullcline. After 120min,
416 the system arrives at the “ \times ” on the c -nullcline (Fig. 7A). Once the stress is shut
417 off the q -nullcline returns to its original position defined by $I = 1$. The trajectory
418 also jumps back horizontally to near the initial q value and subsequently quickly
419 returns to the original upper-branch stable point.

420 External stress induces transition from normal to diseased state

421 We now discuss how transitions from a normal to a diseased state can be induced
422 by *positive* (excitatory) external stress of sufficient duration. In Fig. 8, we start the
423 system in the normal high- c state.

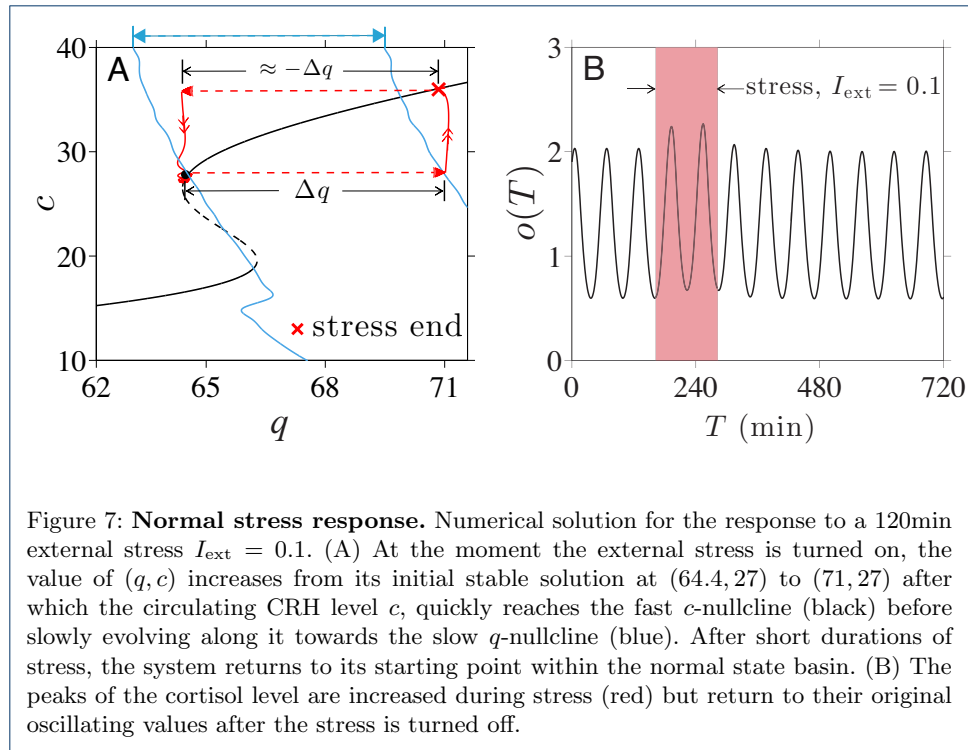
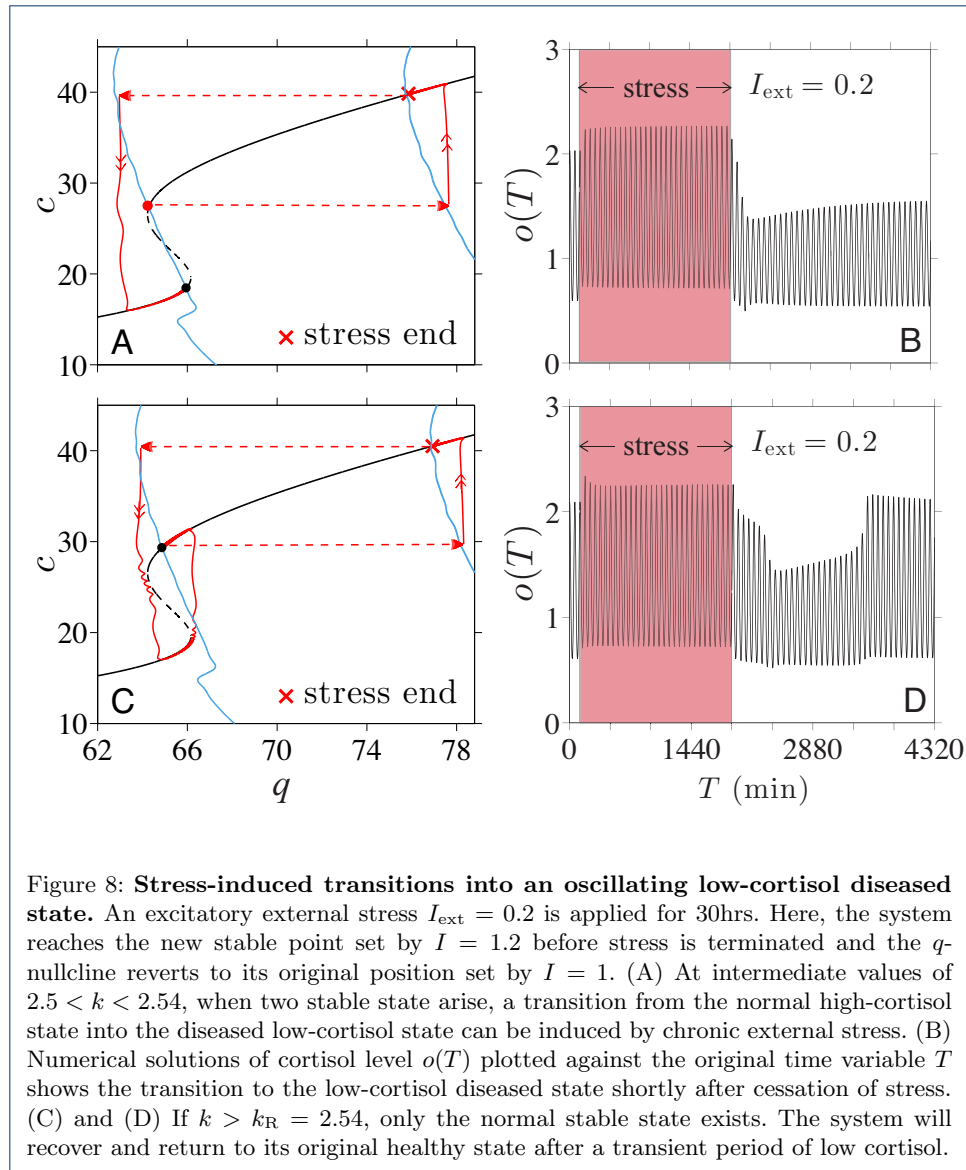


Figure 7: **Normal stress response.** Numerical solution for the response to a 120min external stress $I_{\text{ext}} = 0.1$. (A) At the moment the external stress is turned on, the value of (q, c) increases from its initial stable solution at $(64.4, 27)$ to $(71, 27)$ after which the circulating CRH level c , quickly reaches the fast c -nullcline (black) before slowly evolving along it towards the slow q -nullcline (blue). After short durations of stress, the system returns to its starting point within the normal state basin. (B) The peaks of the cortisol level are increased during stress (red) but return to their original oscillating values after the stress is turned off.

424 Upon stimulation of the CRH neurons through $I_{\text{ext}} > 0$, both CRH and average
 425 glucocorticoid levels are increased while the average value of $c_{\infty}(o(t))$ is decreased
 426 since $c_{\infty}(o)$ is a decreasing function of o . As $c_s(\tau)$ slowly decays towards the de-
 427 creased target value of $\langle c_{\infty}(o(c)) \rangle$, $h(c_s(\tau))$, and hence $q(c_s)$, also decrease. As shown
 428 in Fig. 8A, much of this decrease occurs along the high- c stable branch of the c -
 429 nullcline. Once the external stress is switched off, q will jump back down by a factor
 430 of $1/(1 + I_{\text{ext}})$. If the net decrease in q is sufficient to bring it below the bifurcation
 431 value $q_L \approx 64$ at the leftmost point of the upper knee, the system crosses the sep-
 432 aratrix and approaches the alternate, diseased state. Thus, the normal-to-diseased
 433 transition is more likely to occur if the external stress is maintained long enough to
 434 cause a large net decrease in q , which includes the decrease in q incurred during the
 435 slow relaxation phase, plus the drop in q associated with cessation of stress. The
 436 minimum duration required for normal-to-diseased transition should also depend on
 437 the magnitude of I_{ext} . The relation between the stressor magnitude and duration
 438 will be illustrated in the Additional Files.

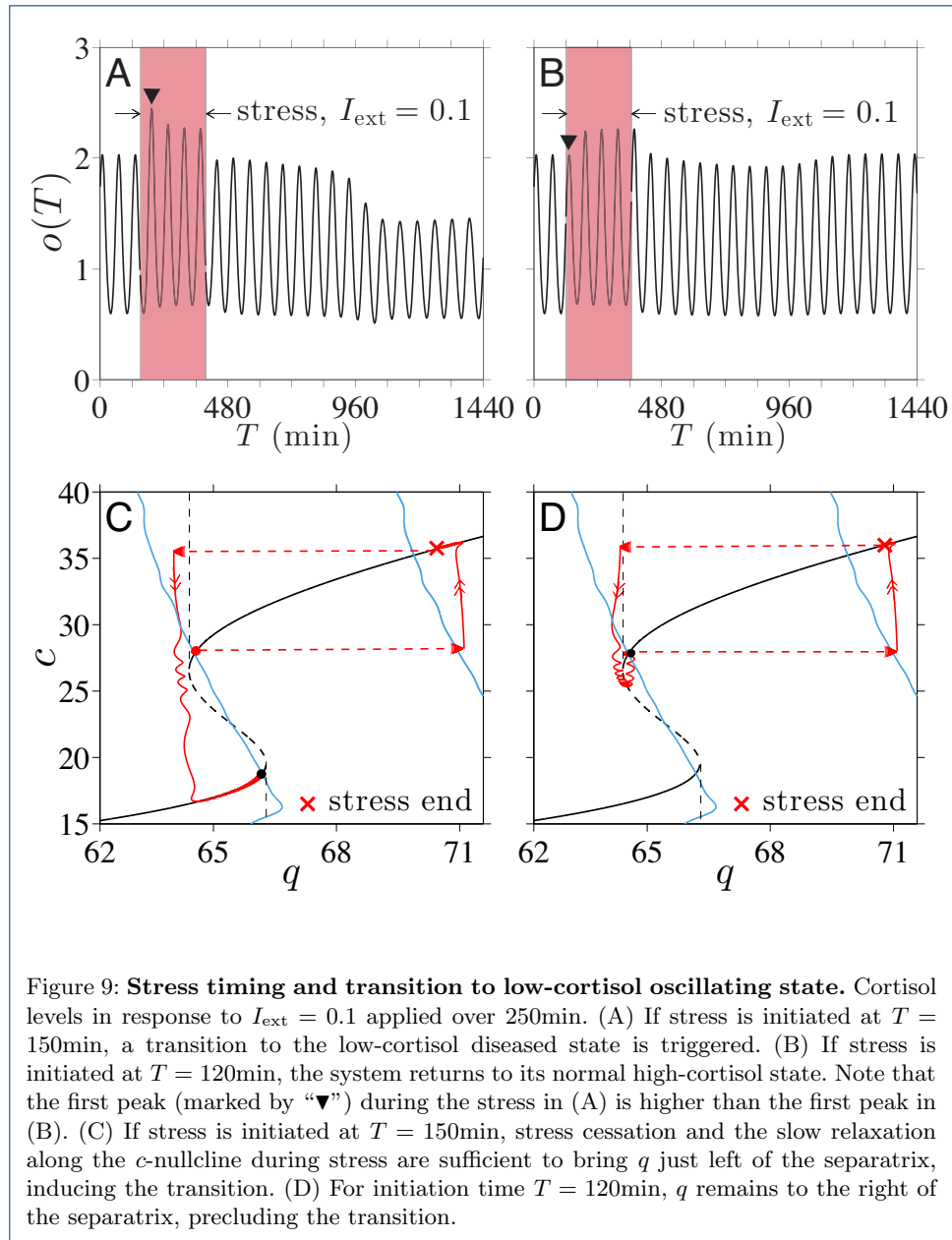
439 A numerical solution of our model with a 30hr $I_{\text{ext}} = 0.2$ was performed, and
 440 the trajectory in (q, c) -space is shown in Fig. 8A. The corresponding cortisol level
 441 along this trajectory is plotted in Fig. 8B, showing that indeed a stable transition
 442 to the lower cortisol state occurred shortly after the cessation of stress. In addition
 443 to a long-term external stress, the stable transition to a diseased state requires
 444 $2.5 < k < 2.54$ and the existence of two stable points. On the other hand, when
 445 $k > k_R = 2.54$, the enhanced CRH release stimulates enough cortisol production to
 446 drive the sole long term solution to the stable upper normal branch of the c -nullcline,
 447 rendering the HPA system *resistant* to stress-induced transitions.



448 The response to chronic stress initially follows the same pattern as described above
 449 for the two-stable-state case, as shown in Fig. 8C. However, the system will continue
 450 to evolve along the lower branch towards the q -nullcline, eventually sliding off the
 451 lower branch near the right bifurcation point (indicated in Fig. S2 by (q_R, c_R))
 452 and returning to the single normal equilibrium state. Thus, when k is sufficiently
 453 high, the system may experience a transient period of lowered cortisol level after
 454 chronic stress but will eventually recover and return to the normal cortisol state. The
 455 corresponding cortisol level shown in Fig. 8D shows this recovery at $T \approx 3400\text{min}$,
 456 which occurs approximately 1500min after the cessation of stress.

457 Transition to diseased state depends on stress timing

458 We have shown how transitions between the oscillating normal and diseased states
 459 depend on the duration of the external stress I_{ext} . However, whether a transition
 460 occurs also depends on the *time* – relative to the phase of the intrinsic ultradian



461 oscillations – at which a fixed-duration external stress is initiated. To illustrate this
 462 dependence on phase, we plot in Figs. 9A and B two solutions for $o(T)$ obtained with
 463 a 250min $I_{\text{ext}} = 0.1$ initiated at different phases of the underlying cortisol oscillation.
 464 If stress is initiated during the rising phase of the oscillations, a transition to the
 465 low-cortisol diseased state occurs and is completed at approximately $T = 1000$ min
 466 (Fig. 9A,C). If, however, stress is initiated during the falling phase, the transition
 467 does not occur and the system returns to the normal stable state (Fig. 9B,D). In
 468 this case, a longer stress duration would be required to push the trajectory past the
 469 low- q separatrix into the diseased state.

470 As discussed earlier, an increase in period-averaged cortisol level during stress
 471 drives a normal-to-diseased state transition. We see that the period-averaged level

472 of cortisol under increased stress is different for stress started at 120min from stress
473 started at 150min. As detailed in the Additional File, the amplitude of the first
474 cortisol peak after the start of stress is significantly lower when the applied stress
475 is started during the falling phase of the intrinsic cortisol oscillations. The differ-
476 ence between initial responses in $o(t)$ affects the period-averaging in $\langle c_\infty(o) \rangle$ during
477 external stress, ultimately influencing c_s and consequently determining whether or
478 not a transition occurs. Note that this phase dependence is appreciable only when
479 stress duration is near the threshold value that brings the system close to the sep-
480 aratrix between normal and diseased basins of attraction. Trajectories that pass
481 near separatrices are sensitive to small changes in the overall negative feedback of
482 cortisol on CRH synthesis, which depend on the start time of the stress signal.

483 Stress of intermediate duration can induce “reverse” transitions

484 We can now use our theory to study how *positive* stressors I_{ext} may be used to
485 induce “reverse” transitions from the diseased to the normal state. Understanding
486 these reverse transitions may be very useful in the context of exposure therapy (ET),
487 where PTSD patients are subjected to stressors in a controlled and safe manner,
488 using for example, computer-simulated “virtual reality exposure.” Within our model
489 we can describe ET as external stress ($I_{\text{ext}} > 0$) applied to a system in the stable
490 low- c diseased state. The resulting horizontal shift in q causes the system to move
491 rightward across the separatrix and suggests a transition to the high- c normal state
492 can occur upon termination of stress. As shown in Fig. 10A, if stressor of sufficient
493 duration is applied, the trajectory reaches a point above the unstable branch of the
494 c -nullcline upon termination leading to the normal, high-cortisol state (Fig. 10B).
495 Since the initial motion is governed by fast flow, the minimum stress duration needed
496 to incite the diseased-to-normal transition is short, on the timescale of minutes.
497 However, if the stressor is applied for too long, a large reduction in q is experienced
498 along the upper stable branch. Cessation of stress might then lower q back into the
499 basin of attraction of the low-cortisol diseased state (Fig. 10C). Fig. 10D shows the
500 cortisol level transiently increasing to a normal level before reverting back to low
501 levels after approximately 1400min.

502 Within our dynamical model, stresses need to be of *intermediate* duration in order
503 to induce a stable transition from the diseased to the normal state. The occurrence
504 of a reverse transition may also depend on the phase (relative to the intrinsic os-
505 cillations of the fast PA subsystem) over which stress was applied, especially when
506 the stress duration is near its transition thresholds. For a reverse diseased-to-normal
507 transition to occur, the decrease in c_s cannot be so large that it brings the trajec-
508 tory past the left separatrix, as shown in Fig. 10C. Therefore, near the maximum
509 duration, stress initiated over the falling phase of cortisol oscillation will be more
510 effective at triggering the transition to a normal high-cortisol state. Overall, these
511 results imply that exposure therapy may be tuned to drive the dynamics of the HPA
512 axis to a normal state in patients with hypocortisolism-associated stress disorders.

513 Summary and Conclusions

514 We developed a theory of HPA dynamics that includes stored CRH, circulating
515 CRH, ACTH, cortisol and glucocorticoid receptor. Our model incorporates a fast

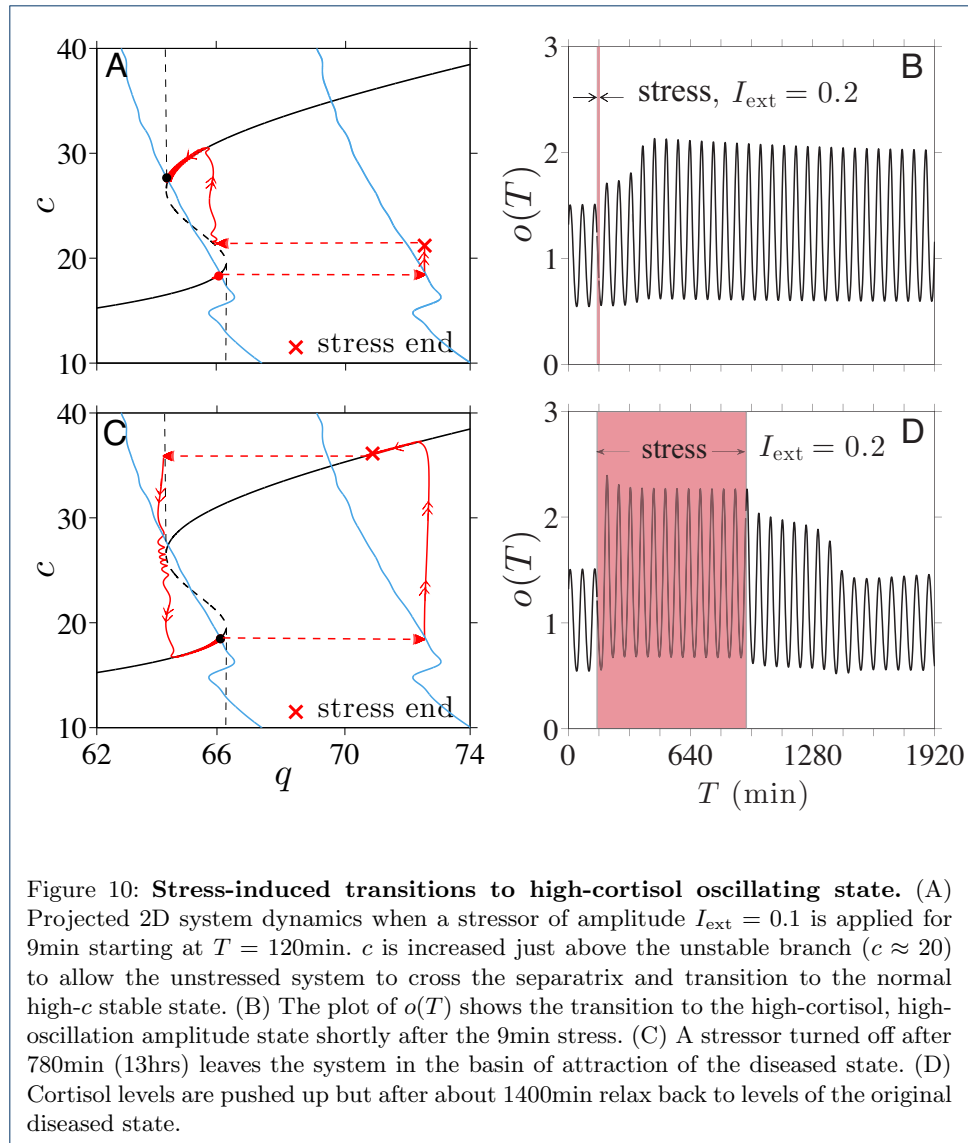


Figure 10: **Stress-induced transitions to high-cortisol oscillating state.** (A) Projected 2D system dynamics when a stressor of amplitude $I_{\text{ext}} = 0.1$ is applied for 9min starting at $T = 120\text{min}$. c is increased just above the unstable branch ($c \approx 20$) to allow the unstressed system to cross the separatrix and transition to the normal high- c stable state. (B) The plot of $o(T)$ shows the transition to the high-cortisol, high-oscillation amplitude state shortly after the 9min stress. (C) A stressor turned off after 780min (13hrs) leaves the system in the basin of attraction of the diseased state. (D) Cortisol levels are pushed up but after about 1400min relax back to levels of the original diseased state.

516 self-upregulation of CRH release, a slow negative feedback effect of cortisol on CRH
 517 synthesis, and a delay in ACTH-activated cortisol synthesis. These ingredients allow
 518 our model to be separated into slow and fast components and projected on a 2D
 519 subspace for analysis.

520 Depending on physiological parameter values, there may exist zero, one, or two
 521 stable simultaneous solutions of both fast and slow variables. For small k , CRH
 522 release is weak and only the low-CRH equilibrium point arises; an individual with
 523 such k is trapped in the low-cortisol “diseased” state. For large k , only the high-CRH
 524 normal state arises, rendering the individual resistant to acquiring the long-term,
 525 low-cortisol side-effect of certain stress disorders. When only one stable solution
 526 arises, HPA dysregulation must depend on changes in parameters resulting from
 527 permanent physiological modifications due to *e.g.*, aging, physical trauma, or stress
 528 itself [46, 47]. For example, it has been observed that older rats exhibit increased
 529 CRH secretion while maintaining normal levels of CRH mRNA in the PVN [48].

530 Such a change could be interpreted as an age-dependent increase in k , which, in
531 our model, implies that aging makes the organism more resistant to stress-induced
532 hypocortisolism. Indeed, it has been suggested that prevalence of PTSD declines
533 with age [49, 50].

534 Other regulatory systems that interacts with or regulate the HPA axis can also
535 affect parameter values in our model. Gonadal steroids, which are regulated by
536 another neuroendocrine system called the hypothalamic-pituitary-gonadal (HPG)
537 axis, activate the preoptic area (POA) of the hypothalamus [51, 52], which in turn
538 attenuates the excitatory effects of medial amygdala stimulation of the HPA axis
539 [53]. Thus, low testosterone levels associated hypogonadism would effectively in-
540 crease $I(t)$ within our model, shift the q -nullcline in the (q, c) -space, and in turn
541 increase cortisol levels. One might consider this as a possible explanation for chron-
542 ically elevated cortisol levels observed in major depressive disorder patients who
543 suffers from hypogonadism. Although it is beyond the scope of this paper, one
544 may further investigate role of gonadal hormones, or role of any other interacting
545 systems, in mediating stress response by considering which parameters would be
546 affected in our model.

547 Within certain parameter regimes and for intermediate k , our theory can also
548 exhibit bistability. When two stable solutions arise, we identify the states with low
549 oscillating levels of cortisol as the diseased state associated with hypocortisolism.
550 Transitions between different stable states can be induced by temporary external
551 stress inputs, implying that HPA dysregulation may develop without permanent
552 “structural” or physiological changes. Stresses that affect secretion of CRH by the
553 PVN are shown to be capable of inducing transitions from normal to diseased states
554 provided they are of sufficient duration (Fig. 8).

555 Our model offers a mechanistic explanation to the seemingly counter-intuitive
556 phenomenon of lower cortisol levels after stress-induced *activation* of cortisol pro-
557 duction. Solutions to our model demonstrate that the negative-feedback effect of
558 a temporary increase in cortisol on the synthesis process of CRH can slowly accu-
559 mulate during the stress response and eventually shift the system into a different
560 basin of attraction. Such a mechanism provides an alternative to the hypothesis that
561 hypocortisolism in PTSD patients results from permanent changes in physiological
562 parameters associated with negative-feedback of cortisol [54, 55].

563 We also find that external stress can induce the “reverse” transition from a dis-
564 eased low-cortisol state to the normal high-cortisol state. Our results imply that
565 re-exposure to stresses of *intermediate* duration can drive the system back to nor-
566 mal HPA function, possibly “decoupling” stress disorders from hypocortisolism.

567 Interestingly, we show that the minimum durations required for either transition
568 depends on the time at which the stress is initiated relative to the phase of the in-
569 trinsic oscillations in (a, o, r) . Due to subtle differences in cortisol levels immedi-
570 ately following stress initiation at different phases of the intrinsic cortisol oscillation, the
571 different cumulative negative-feedback effect on CRH can determine whether or not
572 a trajectory crosses a separatrix (Fig. 9). When the duration of external stress is
573 near its threshold, normal-to-diseased state transitions are easier to induce when
574 stress is initiated during the rising phase of cortisol oscillations. Reverse diseased-
575 to-normal transitions are more easily induced when stress is initiated during the
576 falling phase.

577 In summary, our theory provides a mechanistic picture that connects cortisol dys-
578 regulation with stress disorders and a mathematical framework one can use to study
579 the downstream effects of therapies such as brief eclectic psychotherapy (BEP) and
580 exposure therapy (ET). Both therapies involve re-experiencing stressful situations
581 directly or through imagination, and have been consistently proven effective as
582 first-line treatments for PTSD symptoms [56–58]. Our results suggest that ET can
583 directly alter and “decouple” the expression of cortisol from an underlying upstream
584 disorder. Changes in neuronal wiring that typically occur over slower times scales is
585 also expected after ET [59]. In our model, such changes would lead to slow changes
586 in the basal input $I(t)$. Thus, cortisol level may not be tightly correlated with PTSD,
587 particularly in the context of ET.

588 It is important to emphasize that we modeled neuroendocrine dynamics down-
589 stream of the stress input I_{ext} . How the form of the stress function I_{ext} depends
590 on the type of stress experienced requires a more detailed study of more upstream
591 processes, including how hormones might feedback to these higher-brain processes.
592 Since *higher* cortisol levels are found among female PTSD patients with a history
593 of childhood abuse [60] and among PTSD patients who have experienced a nuclear
594 accident [61], future studies of such divergent, experience-dependent dysregulation
595 will rely on more complex input functions $I_{\text{ext}}(t)$. For example, under periodic
596 driving, complex resonant behavior should arise depending on the amplitude and
597 frequency of the external stress $I_{\text{ext}}(t)$ and the nullcline structure of the specific
598 system. Moreover, effects of other regulatory networks that interacts with the HPA
599 axis can be included in our model through appropriate forms of $I_{\text{ext}}(t)$. For exam-
600 ple, the effects of gonadal steroids in the stress response mentioned above can be
601 further investigated by considering a form of $I_{\text{ext}}(t)$ that is dependent on gonadal
602 steroids level. Many other interesting properties, such as response to dexametha-
603 sone administration, can be readily investigated within our model under different
604 system parameters.

605 **Competing interests**

606 The authors declare that they have no competing interests.

607 **Author’s contributions**

608 **Acknowledgments**

609 This work was supported by the Army Research Office via grant W911NF-14-1-0472 and the NSF through grant
610 BCS-1348123. The authors also thank professors T. Minor and M. Wechselberger for insightful discussions.

611 **Author details**

612 ¹Dept. of Biomathematics, Univ of California, Los Angeles, Los Angeles, USA. ² Department of Mathematics,
613 CalState-Northridge, Los Angeles, USA. ³Dept. of Biomathematics, Univ of California, Los Angeles, Los Angeles,
614 USA.

615 **References**

- 616 1. Denver, R.: Structural and functional evolution of vertebrate neuroendocrine stress systems. *Annals of the New*
617 *York Academy of Sciences* **1163**(1), 1–16 (2009)
- 618 2. Gold, P., Chrousos, G.: Organization of the stress system and its dysregulation in melancholic and atypical
619 depression: high vs low CRH/NE states. *Molecular Psychiatry* **7**(3), 254–275 (2002)
- 620 3. Juruena, M., Cleare, A., Pariante, C.: The hypothalamic pituitary adrenal axis, glucocorticoid receptor function
621 and relevance to depression. *Revista Brasileira de Psiquiatria* **26**(3), 189–201 (2004)
- 622 4. Rohleder, N., Joksimovic, L., Wolf, J., Kirschbaum, C.: Hypocortisolism and increased glucocorticoid sensitivity
623 of pro-inflammatory cytokine production in bosnian war refugees with posttraumatic stress disorder. *Biological*
624 *Psychiatry* **55**(7), 745–751 (2004)
- 625 5. Giorgio, A.D., Hudson, M., Jerjes, W., Cleare, A.: 24-hour pituitary and adrenal hormone profiles in chronic
626 fatigue syndrome. *Psychosomatic Medicine* **67**(3), 433–440 (2005)
- 627 6. Jerjesnd, W., Peters, T., Taylor, N., Wood, P., Wessely, S., Cleare, A.: Diurnal excretion of urinary cortisol,
628 cortisone, and cortisol metabolites in chronic fatigue syndrome. *Journal of Psychosomatic Research* **60**(2),
629 145–153 (2006)

- 630 7. Crofford, L., Young, E., Cary, N.E.K., Korszun, A., Brucksch, C., McClure, L., Brown, M., Demitrack, M.:
631 Basal circadian and pulsatile ACTH and cortisol secretion in patients with fibromyalgia and/or chronic fatigue
632 syndrome. *Brain, Behavior, and Immunity* **18**(4), 314–325 (2004)
- 633 8. Yehuda, R., Teicher, M., Levengood, R., Trestman, R., Siever, L.: Circadian regulation of basal cortisol levels in
634 posttraumatic stress disorder. *Annals of the New York Academy of Sciences* **746**(1), 378–380 (1994)
- 635 9. Vinther, F., Andersen, M., Ottesen, J.T.: The minimal model of the hypothalamic-pituitary-adrenal axis.
636 *Journal of Mathematical Biology* **63**, 663–690 (2011)
- 637 10. Jelic, S., Cupic, Z., Kolar-Anic, L.: Mathematical modeling of the hypothalamic-pituitary-adrenal system activity.
638 *Mathematical Biosciences* **197**, 173–187 (2005)
- 639 11. Kyrlyov, V., Severyanova, L., Vieira, A.: Modeling robust oscillatory behavior of the
640 hypothalamic-pituitary-adrenal axis. *IEEE Transactions on Biomedical Engineering* **52**(12), 1977–1983 (2005)
- 641 12. Savić, D., Knežević, G., Opačić, G.: A mathematical model of stress reaction: Individual differences in threshold
642 and duration. *Psychobiology* **28**(4), 581–592 (2000)
- 643 13. Walker, J.J., Terry, J.R., Lightman, S.L.: Origin of ultradian pulsatility in the hypothalamic-pituitary-adrenal
644 axis. *Proceedings of the Royal Society of London B: Biological Sciences* **277**(1688), 1627–1633 (2010)
- 645 14. Rankin, J., Walker, J., Windle, R., Lightman, S., Terry, J.: Characterizing dynamic interactions between
646 ultradian glucocorticoid rhythmicity and acute stress using the phase response curve. *PLoS One* **7**(2), 30978
647 (2012)
- 648 15. Bairagi, N., Chatterjee, S., Chattopadhyay, J.: Variability in the secretion of corticotropin-releasing hormone,
649 adrenocorticotropic hormone and cortisol and understandability of the hypothalamic-pituitary-adrenal axis
650 dynamics — a mathematical study based on clinical evidence. *Mathematical Medicine and Biology* (2008)
- 651 16. Sriram, K., Rodriguez-Fernandez, M., Doyle III, F.J.: Modeling cortisol dynamics in the neuro-endocrine axis
652 distinguishes normal, depression, and post-traumatic stress disorder (PTSD) in humans. *PLoS Computational*
653 *Biology* **8**, 1002379 (2012)
- 654 17. Gupta, S., Aslakson, E., Gurbaxani, B.M., Vernon, S.D.: Inclusion of the glucocorticoid receptor in a
655 hypothalamic pituitary adrenal axis model reveals bistability. *Theoretical Biology and Medical Modelling* **4**, 8
656 (2007)
- 657 18. Windle, R., Wood, S., Lightman, S., Ingram, C.: The pulsatile characteristics of hypothalamo-pituitary-adrenal
658 activity in female Lewis and Fischer 344 rats and its relationship to differential stress responses. *Endocrinology*
659 **139**(10), 4044–4052 (1998)
- 660 19. Chrousos, G.: Editorial: ultradian, circadian, and stress-related hypothalamic-pituitary-adrenal axis activity — a
661 dynamic digital-to-analog modulation. *Endocrinology* **139**(2), 437–440 (1998)
- 662 20. Conway-Campbell, B., Sarabdjitsingh, R., McKenna, M., Pooley, J., Kershaw, Y., Meijer, O., Kloet, E.D.,
663 Lightman, S.: Glucocorticoid ultradian rhythmicity directs cyclical gene pulsing of the clock gene period 1 in rat
664 hippocampus. *Journal of Neuroendocrinology* **22**(10), 1093–1100 (2010)
- 665 21. Windle, R., Wood, S., Shanks, N., Lightman, S., Ingram, C.: Ultradian rhythm of basal corticosterone release in
666 the female rat: Dynamic interaction with the response to acute stress. *Endocrinology* **139**(2), 443–450 (1998)
- 667 22. Watts, A.: Glucocorticoid regulation of peptide genes in neuroendocrine CRH neurons: a complexity beyond
668 negative feedback. *Frontiers in Neuroendocrinology* **26**(3), 109–130 (2005)
- 669 23. Ono, N., Castro, J.D., McCann, S.: Ultrashort-loop positive feedback of corticotropin (ACTH)-releasing factor
670 to enhance ACTH release in stress. *Proceedings of the National Academy of Sciences* **82**(10), 3528–3531
671 (1985)
- 672 24. FitzHugh, R.: Mathematical models of threshold phenomena in the nerve membrane. *The Bulletin of*
673 *Mathematical Biophysics* **17**(4), 257–278 (1955)
- 674 25. Silva, F.L.D., Blanes, W., Kalitzin, S., Parra, J., Suffczynski, P., Velis, D.: Epilepsies as dynamical diseases of
675 brain systems: basic models of the transition between normal and epileptic activity. *Epilepsia* **44**(s12), 72–83
676 (2003)
- 677 26. Ben-Zvi, A., Vernon, S.D., Broderick, G.: Model-based therapeutic correction of hypothalamic-pituitary-adrenal
678 axis dysfunction. *PLoS Computational Biology* **5**(1), 1000273 (2009)
- 679 27. Tsai, S.Y., Carlstedt-Duke, J., Weigel, N.L., Dahlman, K., Gustafsson, J., M.Tsai, O'Malley, B.W.: Molecular
680 interactions of steroid hormone receptor with its enhancer element: evidence for receptor dimer formation. *Cell*
681 **55**(2), 361–369 (1988)
- 682 28. Andersen, M., Vinther, F., Ottesen, J.: Mathematical modeling of the hypothalamic-pituitary-adrenal gland
683 (HPA) axis, including hippocampal mechanisms. *Mathematical Biosciences* **246**(1), 122–138 (2013)
- 684 29. Papaikonomou, E.: Rat adrenocortical dynamics. *The Journal of Physiology* **265**(1), 119–131 (1977)
- 685 30. Engler, D., Pham, T., Liu, J., Fullerton, M., Clarke, I., Funder, J.: Studies of the regulation of the
686 hypothalamic-pituitary-adrenal axis in sheep with hypothalamic-pituitary disconnection. II. evidence for in vivo
687 ultradian hypersecretion of proopiomelanocortin peptides by the isolated anterior and intermediate pituitary.
688 *Endocrinology* **127**(4), 1956–1966 (1990)
- 689 31. Weiser, M., Osterlund, C., Spencer, R.: Inhibitory effects of corticosterone in the hypothalamic paraventricular
690 nucleus (pvn) on stress-induced adrenocorticotropic hormone secretion and gene expression in the pvn and
691 anterior pituitary. *Journal of Neuroendocrinology* **23**(12), 1231–1240 (2011)
- 692 32. Ma, X., Aguilera, G.: Differential regulation of corticotropin-releasing hormone and vasopressin transcription by
693 glucocorticoids. *Endocrinology* **140**(12), 5642–5650 (1999)
- 694 33. Watts, A., Sanchez-Watts, G.: Region-specific regulation of neuropeptide mRNAs in rat limbic forebrain
695 neurones by aldosterone and corticosterone. *The Journal of Physiology* **484**(3), 721–736 (1995)
- 696 34. Tasker, J., Di, S., Malcher-Lopes, R.: Rapid glucocorticoid signaling via membrane-associated receptors.
697 *Endocrinology* **147**(12), 5549–5556 (2006)
- 698 35. Kasai, M., Yamashita, H.: Inhibition by cortisol of neurons in the paraventricular nucleus of the hypothalamus
699 in adrenalectomized rats; an in vitro study. *Neuroscience Letters* **91**(1), 59–64 (1988)
- 700 36. Kasai, M., Yamashita, H.: Cortisol suppresses noradrenaline-induced excitatory responses of neurons in the
701 paraventricular nucleus; an in vitro study. *Neuroscience letters* **91**(1), 65–70 (1988)

- 702 37. Jones, M., Hillhouse, E., Burden, J.: Dynamics and mechanics of corticosteroid feedback at the hypothalamus
703 and anterior pituitary gland. *Journal of Endocrinology* **73**(3), 405–417 (1977)
- 704 38. Ginsberg, A., Campeau, S., Day, H., Spencer, R.: Acute glucocorticoid pretreatment suppresses stress-induced
705 hypothalamic-pituitary-adrenal axis hormone secretion and expression of corticotropin-releasing hormone
706 hnRNA but does not affect c-fos mRNA or fos protein expression in the paraventricular nucleus of the
707 hypothalamus. *Journal of Neuroendocrinology* **15**(11), 1075–1083 (2003)
- 708 39. Chen, Y., Hua, S., Wang, C., Wu, L., Gu, Q., Xing, B.: An electrophysiological study on the membrane
709 receptor-mediated action of glucocorticoids in mammalian neurons. *Neuroendocrinology* **53**(Suppl. 1), 25–30
710 (1991)
- 711 40. Imaki, T., Xiao-Quan, W., Shibasaki, T., Yamada, K., Harada, S., Chikada, N., Naruse, M., Demura, H.:
712 Stress-induced activation of neuronal activity and corticotropin-releasing factor gene expression in the
713 paraventricular nucleus is modulated by glucocorticoids in rats. *Journal of Clinical Investigation* **96**(1), 231
714 (1995)
- 715 41. Papadimitriou, A., Priftis, K.: Regulation of the hypothalamic-pituitary-adrenal axis. *Neuroimmunomodulation*
716 **16**(5), 265 (2009)
- 717 42. Makino, S., Hashimoto, K., Gold, P.: Multiple feedback mechanisms activating corticotropin-releasing hormone
718 system in the brain during stress. *Pharmacology Biochemistry and Behavior* **73**(1), 147–158 (2002)
- 719 43. Lightman, S., Wiles, C., Atkinson, H., Henley, D., Russell, G., Leendertz, J., McKenna, M., Spiga, F., Wood,
720 S., Conway-Campbell, B.: The significance of glucocorticoid pulsatility. *European Journal of Pharmacology*
721 **583**(2), 255–262 (2008)
- 722 44. Herman, J.P., Figueiredo, H., Mueller, N.K., Ulrich-Lai, Y., Ostrander, M., Choi, D., Cullinan, W.: Central
723 mechanisms of stress integration: hierarchical circuitry controlling hypothalamopituitaryadrenocortical
724 responsiveness. *Frontiers in Neuroendocrinology* **24**(3), 151–180 (2003)
- 725 45. McEwen, B.S., Stellar, E.: Stress and the individual: mechanisms leading to disease. *Arch. Intern. Med.* **153**,
726 2093–2101 (1993)
- 727 46. McEwen, B.S.: Stress, adaptation, and disease: Allostasis and allostatic load. *Annals of the New York Academy*
728 *of Sciences* **840**(1), 33–44 (1998)
- 729 47. Dince, S.M., Rome, R.D., McEwen, B.S., Tang, A.C.: Enhancing offspring hypothalamic-pituitary-adrenal (hpa)
730 regulation via systematic novelty exposure: the influence of maternal HPA function. *Frontiers in Behavioral*
731 *Neuroscience* **8** (2014)
- 732 48. Hauger, R.L., Thiruvikraman, K.V., Plotsky, P.M.: Age-related alterations of hypothalamic-pituitary-adrenal axis
733 function in male Fischer 344 rats. *Endocrinology* **134**(3), 1528–1536 (1994)
- 734 49. Averill, P., Beck, J.: Posttraumatic stress disorder in older adults: a conceptual review. *Journal of Anxiety*
735 *Disorders* **14**(2), 133–156 (2000)
- 736 50. Regier, D., Boyd, J., Burke, J., Rae, D., Myers, J., Kramer, M., Robins, L., George, L., Karno, M., Locke, B.:
737 One-month prevalence of mental disorders in the united states: based on five epidemiologic catchment area
738 sites. *Archives of General Psychiatry* **45**(11), 977–986 (1988)
- 739 51. Simerly, R.B., Swanson, L.W., Chang, C., Muramatsu, M.: Distribution of androgen and estrogen receptor
740 mrna-containing cells in the rat brain: An in situ hybridization study. *Journal of Comparative Neurology* **294**(1),
741 76–95 (1990)
- 742 52. Gréco, B., Allegretto, E., Tetel, M., Blaustein, J.: Coexpression of ER β with ER α and progesterin receptor
743 proteins in the female rat forebrain: effects of estradiol treatment. *Endocrinology* **142**(12), 5172–5181 (2001)
- 744 53. andN. Conforti, S.F., Saphier, D.: The preoptic area and bed nucleus of the stria terminalis are involved in the
745 effects of the amygdala on adrenocortical secretion. *Neuroscience* **37**(3), 775–779 (1990)
- 746 54. Yehuda, R., Teicher, M., Levengood, R., Trestman, R., Levengood, R., Siever, L.: Cortisol regulation in
747 posttraumatic stress disorder and major depression: a chronobiological analysis. *Biological Psychiatry* **40**(2),
748 79–88 (1996)
- 749 55. Yehuda, R., LeDoux, J.: Response variation following trauma: a translational neuroscience approach to
750 understanding PTSD. *Neuron* **56**, 19–32 (2007)
- 751 56. Olf, M., de Vries, G., Güzelcan, Y., Assies, J., Gersons, B.: Changes in cortisol and DHEA plasma levels after
752 psychotherapy for PTSD. *Psychoneuroendocrinology* **32**(6), 619–626 (2007)
- 753 57. Foa, E., Keane, T., Friedman, M., Cohen, J.: Effective treatments for PTSD: practice guidelines from the
754 international society for traumatic stress studies (2008)
- 755 58. Rauch, S., Eftekhari, A., Ruzek, J.: Review of exposure therapy: a gold standard for PTSD treatment. *The*
756 *Journal of Rehabilitation Research and Development* (49), 679–88 (2012)
- 757 59. Trouche, S., Sasaki, J., Tu, T., Reijmers, L.: Fear extinction causes target-specific remodeling of perisomatic
758 inhibitory synapses. *Neuron* **80**(4), 1054–1065 (2013)
- 759 60. Lemieux, A., Coe, C.: Abuse-related posttraumatic stress disorder: evidence for chronic neuroendocrine
760 activation in women. *Psychosomatic Medicine* **57**(2), 105–115 (1995)
- 761 61. Baum, A.: Implications of psychological research on stress and technological accidents. *American Psychologist*
762 **48**(6), 665 (1993)
- 763 62. Schürmeyer, T.H., Avgerinos, P.C., Gold, P.W., Gallucci, W.T., Tomai, T.P., Jr, G.B.C., Loriaux, D.L.,
764 Chrousos, G.P.: Human corticotropin-releasing factor in man: pharmacokinetic properties and dose-response of
765 plasma adrenocorticotropin and cortisol secretion. *The Journal of Clinical Endocrinology & Metabolism* **59**(6),
766 1103–1108 (1984)

767 **Tables**

Table S1: Dimensionless parameter values of our full model. Analogous parameters from the literature are referenced.

Parameter	Value	Source and Ref.	Description
n	5	assumed	Hill coefficient in upregulation function $g_c(c)$
\bar{c}_∞	0.2	estimated from [22]	baseline stored CRH level
b	0.56	estimated from [22]	relates cortisol to stored CRH level
k	undetermined	.	relates stored CRH to CRH release rate
μ_c	undetermined	.	basal CRH release rate
q_0	undetermined	.	maximum CRH release rate
q_1^{-1}	undetermined	.	circulating CRH for half-maximum self-upregulation
q_2	1.8	estimated from [21]	ratio of CRH and cortisol decay rates
p_2^{-1}	0.067	p_2^{-1} [43]	(<i>or</i>)-complex level for half-maximum feedback
p_3	7.2	p_3 [43]	ratio of ACTH and cortisol decay rates
p_4	0.05	p_4 [43]	(<i>or</i>)-complex level for half-maximum upregulation
p_5	0.11	p_5 [43]	basal GR production rate by pituitary
p_6	2.9	p_6 [43]	ratio of GR and cortisol decay rates
t_c	69.3	assumed	CRH biosynthesis timescale
t_d	1.44	" τ " [43]	delay in ACTH-activated cortisol release

768 **Additional Files**

769 **Nondimensionalization**

770 Our equations are nondimensionalized in a manner similar to that used by Walker *et al.* [13]:

$$\begin{aligned} t &= d_O T, & c_s &= C_s / \bar{C}_s, & c &= \mu_{RP} d_O C, \\ a &= \mu_{RP} d_O^2 A, & r &= \mu_{RP} d_O R, & o &= \mu_{RP} p_A p_O d_O^3 O, \end{aligned} \quad (\text{A1})$$

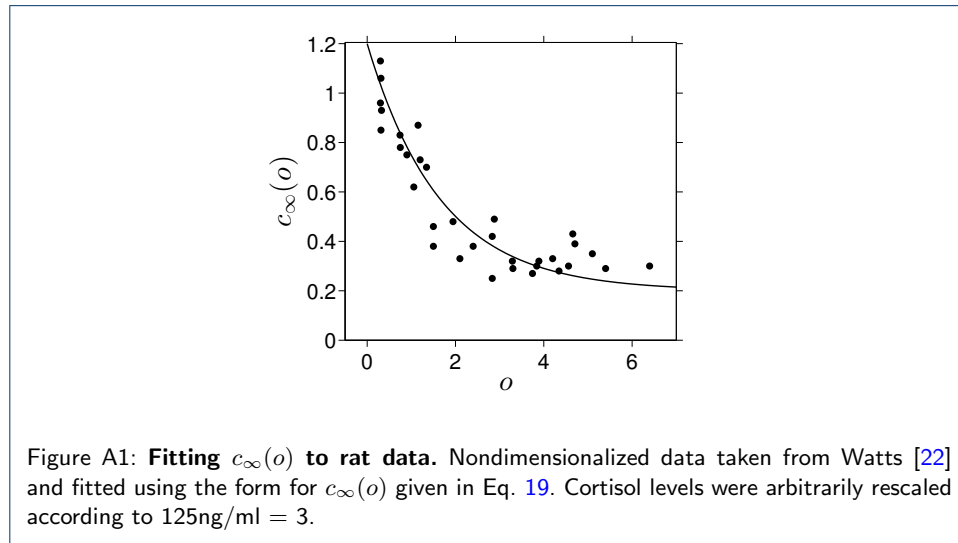
Here, c_s, c, a, r, o are the dimensionless versions of the original concentrations C_s, C, A, R, O , respectively. C_s is normalized by \bar{C}_s , which denotes the typical maximum amount of releasable CRH in the physiological range. Upon using these variables, the dimensionless forms of Eqs. 9-13 are expressed in Eqs. 14-18. The parameters q_i, p_i are dimensionless combinations conveniently defined to be analogous to those used by Walker *et al.* [13]:

$$\begin{aligned} t_c &= d_O T_C, & t_d &= d_O T_d, & q_0 &= p_C / (\mu_{RP} R), \\ q_2 &= d_C / d_O, & p_2 &= \mu_{RP}^2 p_A p_O / (d_O^4 K_A), & p_3 &= d_A / d_O, \\ p_4 &= p_C^4 p_A p_O d_O^8 K_R^2 / \mu_{RP}, & p_5 &= 1 / \mu_{RP}, & p_6 &= d_R / d_O. \end{aligned} \quad (\text{A2})$$

771 Using these scalings, we arrive at the dimensionless Eqs. 14-19.

772 **Parameter estimates**

773 Many of the numerous physiological parameters in our model can be estimated or constructed from previous studies
774 on the HPA axis. For example, as shown in Fig. A1, the parameters forming the function $c_\infty(o)$ are derived from
fitting to data on adrenalectomized male rats [22]. From the fitting, we estimate the baseline level $\bar{c}_\infty \simeq 0.2$, and



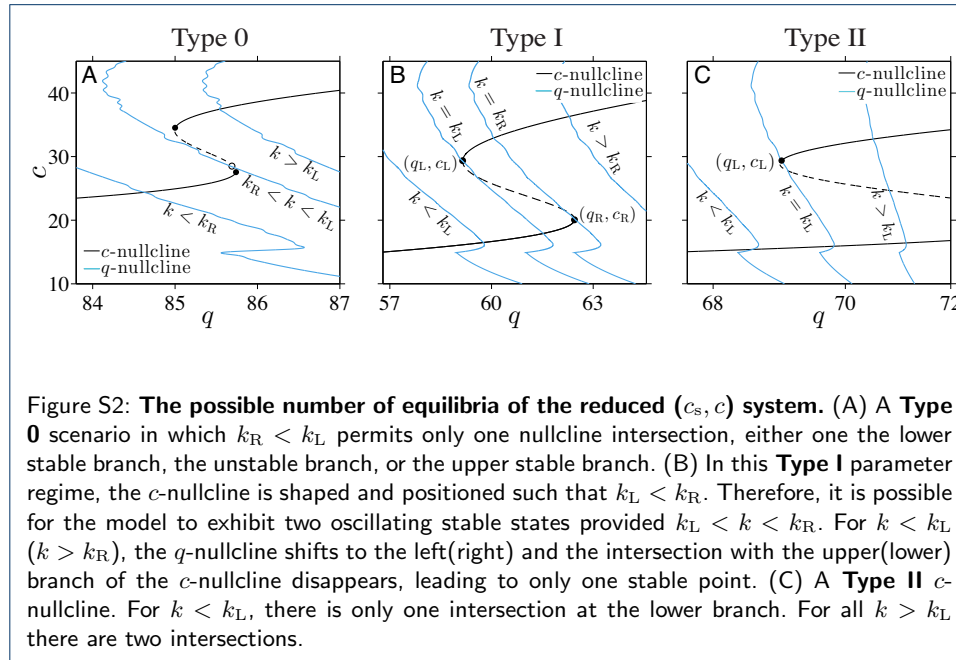
775 the decay rate $b \simeq 0.6$ [22]. Furthermore, the dimensionless parameters p_2, \dots, p_5 and t_d will be fixed to those
776 used in Walker *et al.* [13]: $p_2 = 15, p_3 = 7.2, p_4 = 0.05, p_5 = 0.11, p_6 = 2.9$ and $t_d = 1.44$ ($T_d = 15$ min).
777 Although it is not possible to determine all of the remaining parameters from data, we will use reasonable estimates.
778 The half-life of cortisol was estimated to be about 7.2min [21] while the half-life of CRH has been estimated to be
779 about 4min [62]. Therefore, $q_2 = d_C d_O^{-1} \approx 1.8$. Of the remaining parameters (n, μ_c, q_0, q_1, k), the dependence
780 on n will turn out to be quantitative so we henceforth set $n = 5$. These estimated parameters are listed in Table S1.
781 Even though one expects the values of these effective parameters to be highly variable, we fix them in order to
782 concretely investigate the mathematical structure and qualitative predictions of our model. The parameters $\mu_c, q_0,$
783 $q_1,$ and k remain undetermined; however, it is instructive to treat k as a control parameter and explore the nullcline
784 structure in μ_c, q_0, q_1 parameter space.
785

786 **Parameter space and nullcline structure**

787 To determine how the q -nullcline crosses the c -nullcline, we substitute c_s by its equilibrium period-averaged value
788 $\langle c_\infty(c) \rangle$. If we assume a basal input level $I = 1$, the values of k that will position the basal q -nullcline to just pass
789 through the left and right bifurcation points (q_L, c_L) and (q_R, c_R) can be found by solving
790 $q_{L,R} = q_0 (1 - e^{-k \langle c_\infty(c_{L,R}) \rangle})$:

$$k_L = \frac{1}{\langle c_\infty(c_L) \rangle} \ln \left(\frac{1}{1 - q_L / q_0} \right), \quad k_R = \frac{1}{\langle c_\infty(c_R) \rangle} \ln \left(\frac{1}{1 - q_R / q_0} \right). \quad (\text{A3})$$

All possible ways in which the nullclines can cross each other as k is varied are illustrated in Fig. S2.



791

The specific locations of the bifurcation points, as well as k_L and k_R , are complicated functions of all parameters. However, Eqs. A3 allows us to distinguish three qualitatively different regimes. The first possibility is $k_L > k_R$, where there can be at most only one intersection between the slow and fast nullclines. We denote this as a **Type 0** scenario (Fig. S2A) characterized by having at most a single stable state towards which the system will always return upon cessation of external stress. In Type 0 situations with intermediate values of k , the intersection will arise in the unstable branch of the c -nullcline. In this case, we expect the system to oscillate between the two stable branches of the c -nullcline. Here, the fast variables a , o , and r will cycle periodically between two oscillating levels. In order for the two nullclines to intersect three times (twice on stable branches of the c -nullcline), the q -nullcline must “fit” within the bistable region of the c -nullcline. As shown in Fig. S2, there are two separate subcases of nullclines that intersect twice. If $k_L < k_R$, a value of $k_L < k < k_R$ would imply that the q -nullcline can intersect both stable branches of the c -nullcline, leading to two stable solutions. We refer to this case as **Type I** (Fig. S2B). Another possibility is that the right bifurcation point is beyond the maximum value $q = q_0$ dictated by the function $h((c_\infty(c_R)))$. As shown in Fig. S2C, the bistable c -nullclines exhibits only one bifurcation point within the domain of q . The lower branch of the c -nullclines in this set extends across the entire range of physiological values of q , ensuring that the q -nullcline will intersect with the lower branch for any value of k . Therefore, to determine if there are two intersections we only need to check that $k_L \leq k$ is satisfied. In this **Type II** case, the system is either perpetually in the diseased low cortisol state, or is bistable between the diseased and normal states; the system will always be at least susceptible to low-cortisol disease. Summarizing,

810

- **Type 0**: Exactly one solution (one nullcline intersection) exists for the reduced subsystem. Here, $k_R < k_L$ and the intersection may occur on the lower or upper stable branches, or on the unstable branch of the c -nullcline. The system is either permanently diseased, permanently resistant, or oscillates between normal and diseased states.

814

- **Type I**: At least one solution exists. A stable diseased solution exists if $k < k_L$, two stable solutions (diseased and normal) arise if $k_L \leq k \leq k_R$, and fully resistant state arises if $k > k_R$.

815

- **Type II**: At least one solution exists. A stable diseased state arises if $k < k_L$ while both diseased and normal solutions arise if $k > k_L$. A fully disease-resistant state cannot arise.

816

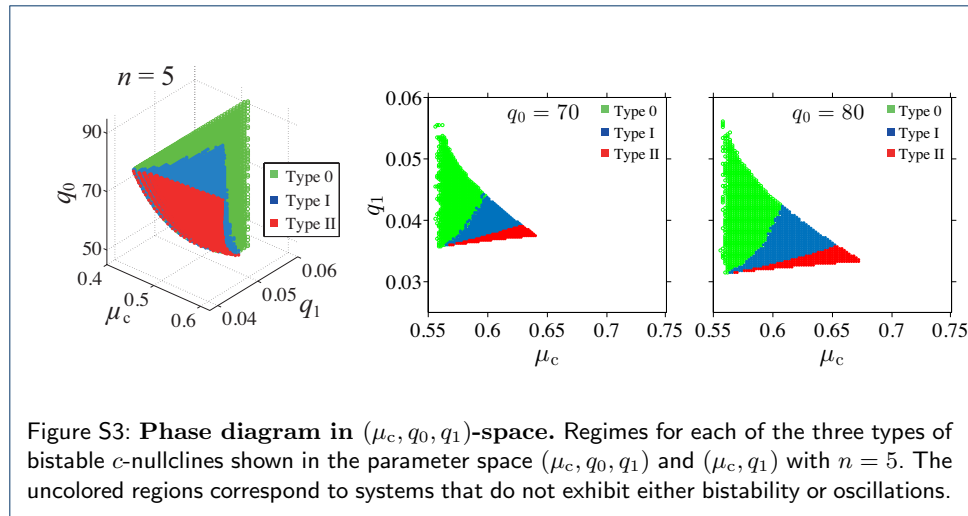
817

With the parameters fixed according to Table S1, we will treat k as a control parameter and exhaustively sweep the three-dimensional parameter space (q_0, q_1, μ_c) to determine the regions which lead to each of the nullcline structural types. In addition, we restrict the parameter domain to regions which admit oscillating solutions of the full problem. In other words, parts of both stable branches of the c -nullclines must fall within values of c which support oscillations in the PA-subsystem (Fig. 3). The regions in (μ_c, q_0, q_1) space that satisfy these conditions and that yield each of the types of nullcline crossings are indicated in Fig. S3.

824

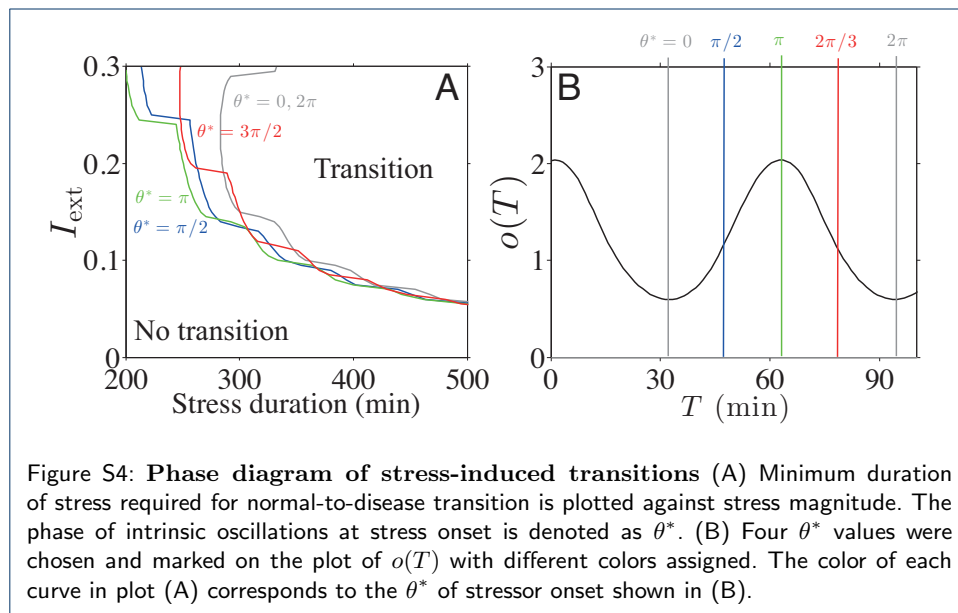
Based on measurements of self-upregulation of CRH secretion during stress [23], $\mu_c = 0.6$ is chosen to set the baseline level of the Hill function $g_c(c = 0) \approx 0.4$. q_1 is approximated by setting the inflection point of $g_c(c)$ to arise at $c \approx 25$, the average value used by Walker *et al.* [13]. Assuming $c \approx 25$ is a fixed point of Eq. 15 when $I = 1$ and $c_s \approx \langle c_\infty(25) \rangle$, q_0 can be estimated as a root of the right-hand-side of Eq. 15. This choice for the remaining parameters puts our nullcline system into the **Type I** category that can exhibit one or two stable states with oscillating (a, o, r) subsystems. We restricted the analysis of our model to **Type I** systems.

829



830 **Minimum duration and magnitude of stress**

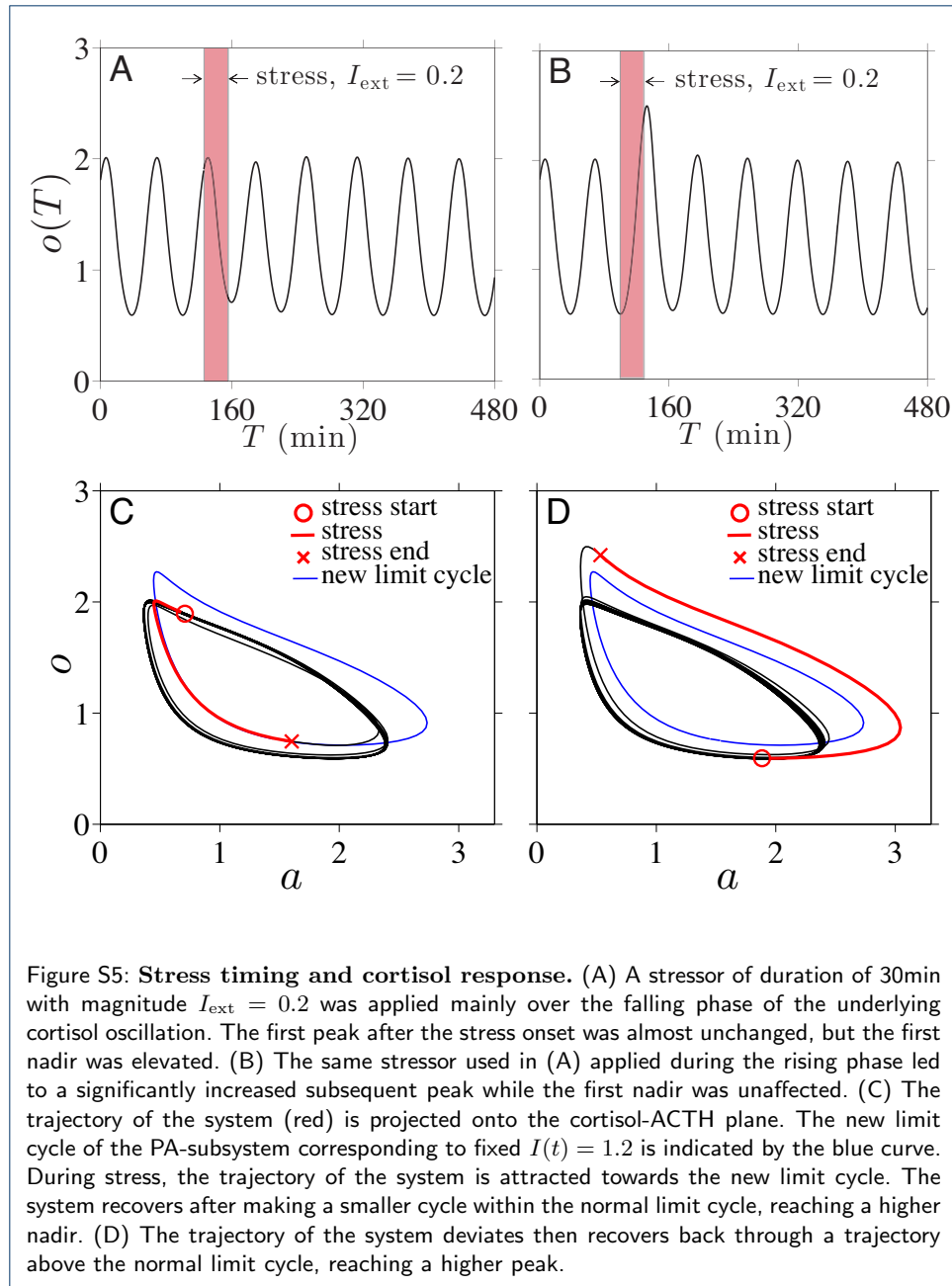
831 We plot the minimum duration required for normal-to-diseased transition against stress magnitude (Fig. S4). Higher
 832 magnitude of I_{ext} generally requires a shorter duration of stress, as expected. Note that the minimum duration is
 833 also dependent on the phase of intrinsic oscillations of the system at stress onset.



834 **Timing of stress onset and transient response**

835 Here, we show how the dynamics of the system changes after the onset and cessation of stress. In previous studies
 836 [18, 21], changes in corticosterone levels in rats were measured in response to stress induced by noise applied at
 837 different phases of the animals oscillating cortisol cycle. It was observed that the timing of the stress onset relative
 838 to the ultradian phase was crucial in determining the magnitude of corticosterone response. Increases in
 839 corticosterone levels were markedly higher when noise was initiated during the rising phase than when initiated
 840 during the falling phase.

841 We can frame these experimental observations mechanistically within our theory. Following the experimental
 842 protocol [18, 21], we simulate the stress response using a brief stressor with a duration of 30min. As shown in
 843 Fig. S5A, an external stress that is applied mostly over the falling phase of the cortisol oscillation results in a higher
 844 subsequent nadir in $o(t)$ than one that is applied predominantly during a rising phase. However, as shown in
 845 Fig. S5B, stress applied mainly during the rising phase leads to a higher subsequent peak level. This observation is
 846 consistent with the results of the experiment on rats and can be explained by the dynamics inherent in our model.
 847 The immediate increase in $q = q_0 I h(c_s)$ associated with the increase in I leads to a rapid increase in c , as shown
 848 in Fig. 7. This higher level of circulating CRH shifts the stable limit cycle of the PA subsystem to a new one with



849 higher minimum and maximum values of ACTH and cortisol (as shown in Fig. 3). This new limit cycle is shown by
 850 the blue curve in Figs. S5C,D. Under external stress, a trajectory of the system quickly deviates and approaches the
 851 new limit cycle, but quickly returns to the original limit cycle after cessation of stress. Thus, depending on the
 852 position of the trajectory relative to that of the new stressed limit cycle, the initial deviation may try to reach the
 853 new limit cycle in the falling or rising cortisol phases as shown in Figs. S5C,D. Moreover, if the duration of the stress
 854 is shorter than the period of the inherent oscillation, the trajectory will return to its original limit cycle before
 855 completing a full cycle of the new limit cycle. These properties of the limit cycle dynamics explain the difference in
 856 the level of subsequent peak following the stress onset depending on the timing of the stress onset.

857 Cortisol dependent I_{ext}

858 As it has been shown that synaptic input of the PVN cells is modulated by cortisol for certain types of stressor, we
 859 briefly discuss how cortisol dependent $I_{\text{ext}}(T, O)$ may affect the behavior of our model. Within our model,
 860 modulation in synaptic input by glucocorticoids can be viewed as a cortisol dependent external input function:
 861 $I_{\text{ext}}(T, O) = I_{\text{time}}(T) + I_{\text{cort}}(O)$. One possible form of $I_{\text{ext}}(T, O)$ is illustrated in Fig. S6 where $I_{\text{ext}}(T, O)$ is
 862 assumed to be lower when cortisol levels are higher. Since it was shown that cortisol does not affect the basal

863 release rate [37], the cortisol dependent component of the external input function, $I_{cort}(O)$, should be zero when
864 there is no stress. On the other hand, it was also shown that the inhibition effect cannot decrease the release rate
865 below the basal rate [37] so we can further assume that $I_{ext}(O, T) \geq 0$. When these conditions are met, the
866 modification in $I_{ext}(T, O)$ should not affect the bistability of the system since $I(T) = I_{base} = 1$ is unchanged.
867 However, a cortisol dependent $I_{ext}(T, O)$ will make the timing of stress onset become more relevant in predicting
868 whether or not stressors can induce transitions between normal and diseased states. Driven by the intrinsic
869 oscillations in $O(T)$, $I_{ext}(T)$ will also oscillate during stress, leading the q -nullcline to shift back and forth during
870 stress in the (q, c) -plane as shown in Fig. S6C. Oscillations in the q -nullcline affect the net decrease in q during
871 stress, changing the position of the system on the (q, c) -plane relative to the separatrix between the normal and the
872 diseased basins of attraction at stress termination.

